Supporting Information

Novel Carbazole-Based Ionic Liquids and Their Charge-Transfer Kinetics Pertaining to Marcus Theory Towards Highly Efficient Redox Active Electrolytes

Kulika Pithaksinsakul[a], Tobias Burton[a], Chayaporn Pareseecharoen[a], Siraprapha Deebansok[a],Vinich Promarak[b], and Olivier Fontaine[a]*,

[a.] Molecular Electrochemistry for Energy Laboratory, School of Energy Science and Engineering, Vidyasirimedhi Institute of Science and Technology, Wangchan, Rayong, 21210, Thailand

[b.] School of Molecular Science and Engineering, Vidyasirimedhi Institute of Science and Technology, Wangchan, Rayong, 21210, Thailand

Contents

General Information

Reagents: reacgents for reactions were purchased as reagent (AR) grade and used without further purification. Bromoethane, carbazole, 2-chloro-2-methylpropane, tetrabutylammonium bromide, bis(trifluoromethane)sulfonimide lithium salt, sodium *tert*-butoxide, 1,3-propane sultone, oxalyl chloride, trifluoromethanesulfonamide and dry lithium hydroxide were purchased from Tokyo Chemical Industry (TCI), zinc chloride from UNILAB, 1,2-dichloroethane from Univar and N-methylimidazole from Acros organics. The reagents were purchased from CARLO ERBA reagents as analysis grade *i.e.,* potassium carbonate, potassium hydroxide and sodium sulfate. Silica gel 60 (0.063-0.200 mm) for column chromatography was purchased from Merck Millipore.

Solvents: solvents for reactions were purchased as reagent (AR) grade from Acros Organics, Carlo Erba, QRëC, and Univar *i.e.,* toluene, nitromethane, dimethylformamide, acetonitrile and 1,2-dichloroethane. In case of dry reactions and electrochemistry part, the solvents were dried through fractionation distillation over sodium hydride and kept in a dry condition with 3A molecular sieves under argon atmosphere. Solvents used in purification were purchased as commercial grade *i.e.,* ethyl acetate, dichloromethane, ethanol, ethyl acetate and methanol. The solvents were purified by rotary vacuum evaporators before use. The water used was purified by a Milli-Q purification system.

Instrument: NMR measurements were performed using BRUKER model of AVANCE III HD (600 MHz). FT-IR spectra were obtained using a Model/Brand of AVANCE III HD (600 MHz) / BRUKER in the ATR mode. Mass spectrometry analyses were carried out on a Model/Brand of Compact QTOF / Bruker. An APCI source was used for low polarity molecules and for quick analysis. An ESI source was performed for high polarity molecules. Thermal gravimetric analysis (TGA) was carried out using Rigaku with the condition of heat from 0–800 °C, heating rate 10 °C/min under argon atmosphere. Differential scanning calorimetry (DSC) measurements were carried out twice cycle on a Model/Brand of Lab System - DSC 8500 / PerkinElmer with the condition of heat from 30 to 10 °C before the onset temperature, heating rate 10 °C/min under argon atmosphere.

Palmsens4 as a potentiostat. Two types of working electrodes were used: a millimeter-sized glassy carbon electrode and an ultra-microelectrode (25 μm of platinum electrode). Before each measurement, the working electrode was polished with 0.05 μm alumina powder and washed with

water and acetone. Silver wire was used as the reference electrode and platinum wire was used as the counter electrode. Cells were assembled in the glovebox and experiments were carried at 25°C under argon atmosphere.

Synthetic methodologies
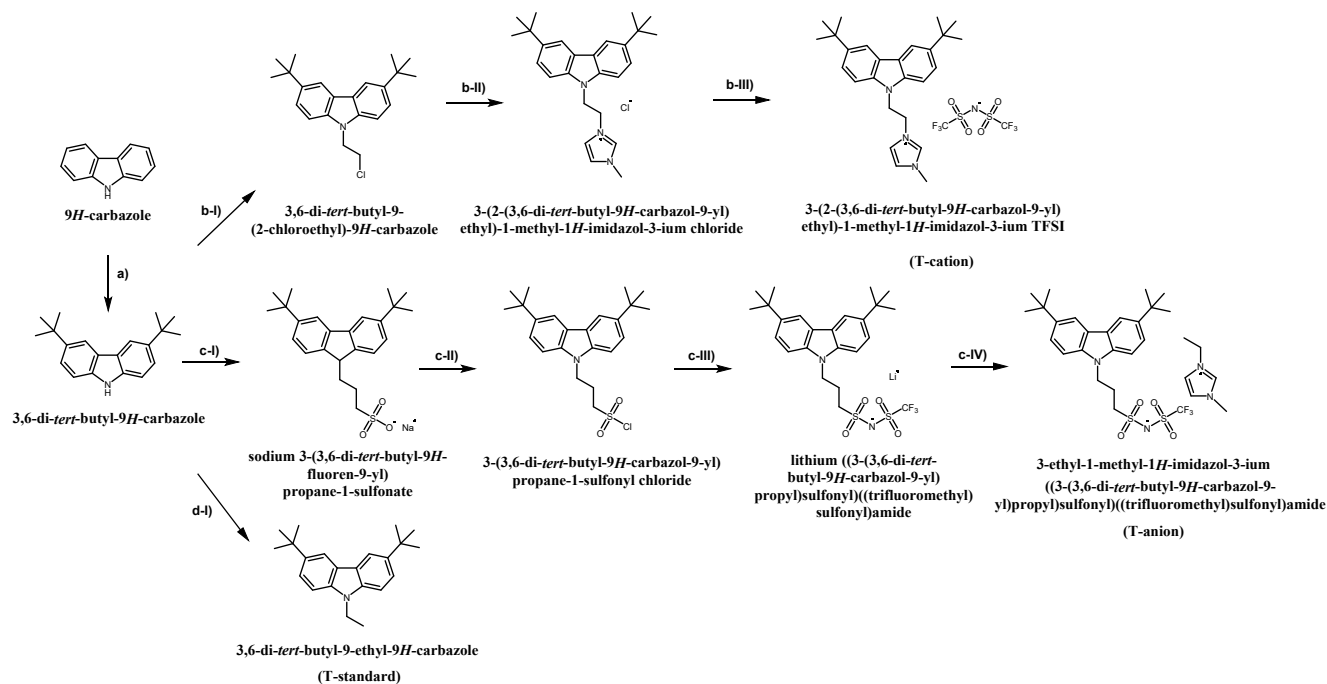
S 1 The overview reaction scheme of the target molecules *i.e.*, 3-(2-(3,6-di-*tert*-butyl-9*H*-carbazol-9-yl)ethyl)-1-methyl-1*H*-imidazol-3-ium *TFSI* (*T-cation*), 3-ethyl-1-methyl-1*H*-imidazol-3-ium (((3-(3,6-di-*tert*-butyl-9*H*-carbazol-9-yl)propyl)sulfonyl)methyl)(((2,2,2-trifluoroethyl)sulfonyl)methyl)amide (*T-anion*), and 3,6-di-*tert*-butyl-9-ethyl-9*H*-carbazole (*T-standard*), based 3,6-di-*tert*-butyl-9*H*-carbazole. A numerous quantity of the based was synthesized as a starting material to produce *T-cation*, *T-anion*, and *T-standard* following route b, c, and d, respectively.

The 3 target molecules of the cation, the anion, and the standard were synthesized as electrolytes. These were illustrated in scheme 1, the 3 target molecules which were synthesized from the modified carbazole, *i.e.,* 3,6-di-*tert*-butyl-9*H*-carbazole-based.

**Synthesis of 3-ethyl-1-methyl-1*H*-imidazol-3-ium bromide**
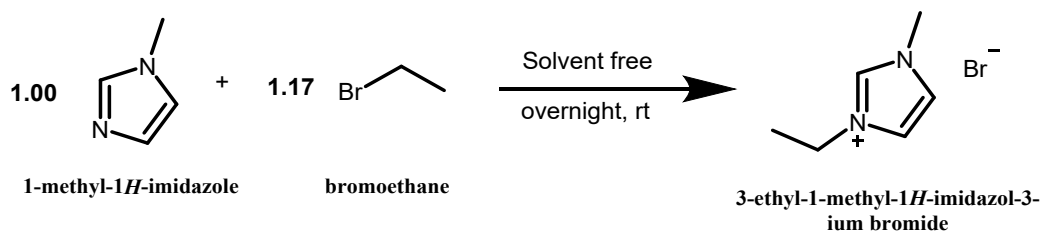
S 2 Synthesis of 3-ethyl-1-methyl-1*H*-imidazol-3-ium bromide

In a single-necked flask equipped with a stir bar were loaded N-methylimidazole (1.5 g, 0.018 mol) and bromoethane (2.29 g, 0.021 mol, 1.17 equiv) [1]. This was then mixed at room temperature overnight. The resulting white precipitate was filtered and washed with ethyl acetate (3 x 20 mL) as to remove any unreacted reagent. The salt was then dried in vacuo yielding the target compound as a white solid.

^{1}H NMR (600 MHz, DMSO) δ (ppm) 9.25 (s, 1H), 7.83 (s, 1H), 7.74 (s, 1H), 4.22 (q, J = 7.3, 2H), 3.87 (s, 3H), 1.42 (t, J = 7.3, 3H); ^{13}C NMR (600 MHz, DMSO) δ (ppm) 136.75, 124.02, 122.45, 44.59, 36.20, 15.61.
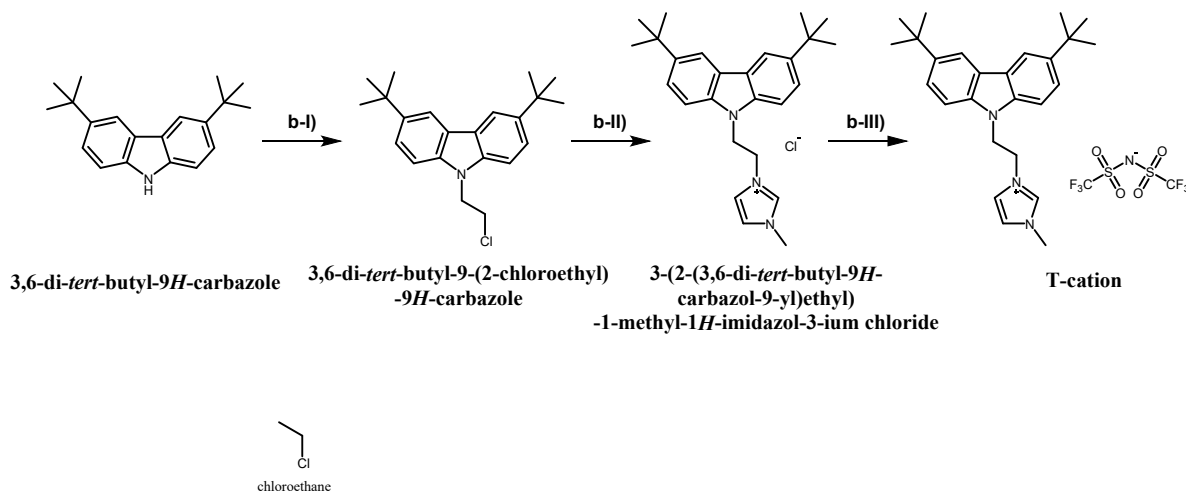
Synthesis of 3,6-di-*tert*-butyl-9*H*-carbazole
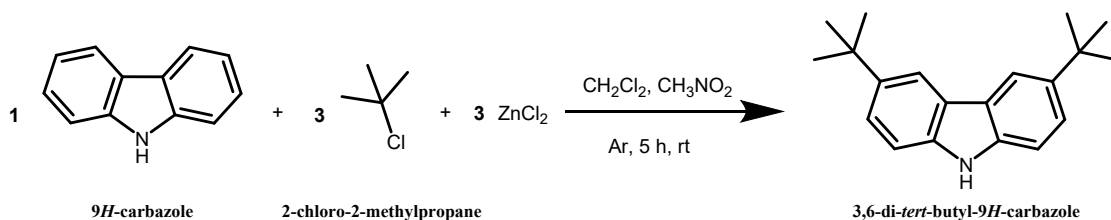
S 3 Synthesis of 3,6-di-*tert*-butyl-9*H*-carbazole

This was adapted from the procedure of Jürgens *et al* [12]. Into a 250 mL round-bottom flask was charged with a commercial carbazole (10 g, 59.81 mol), zinc chloride (24.46 g, 179.42 mol, 3 equiv), and 75 mL of nitromethane under argon atmosphere. During vigorous stirring, 2-chloro-2-methylpropane (16.33 g, 179.42 mol, 3 equiv) was added dropwise and stirred for 1 h. The flask was then transferred into a cooled ultrasound bath and sonicated for 1h. 50 mL of water was then added, and the organic phase was extracted with CH_2Cl_2 (3 x 50 mL). The organic was then dried with sodium sulfate and the solvent was removed in the rotary evaporator yielding a brown solid. This solid was recrystallized four times in a CH_2Cl_2:MeOH (20:80) to yield golden colored crystals of the target 3,6-di-*tert*-butyl-*9H*-carbazole.

^{1}H NMR (600 MHz, CDCl$_3$): δ (ppm) 8.09 (s, 2H), 7.82 (s, 1H), 7.47 (d, J = 8.22 Hz, 2H), 7.33 (d, J = 8.34 Hz, 2H), 1.47 (s, 18H); ^{13}C NMR (600 MHz, CDCl$_3$) δ (ppm) 142.4, 138.2, 123.6, 116.3, 110.2, 34.8, 36.2.

Synthesis of 3-(2-(3,6-di-*tert*-butyl-9*H*-carbazol-9-yl)ethyl)-1-methyl-1*H*-imidazol-3-ium TFSI (*T-cation*)

S 4 The overview reaction scheme of synthesis of 3-(2-(3,6-di-*tert*-butyl-9*H*-carbazol-9-yl)ethyl)-1-methyl-1*H*-imidazol-3-ium *TFSI* (***T-cation***)

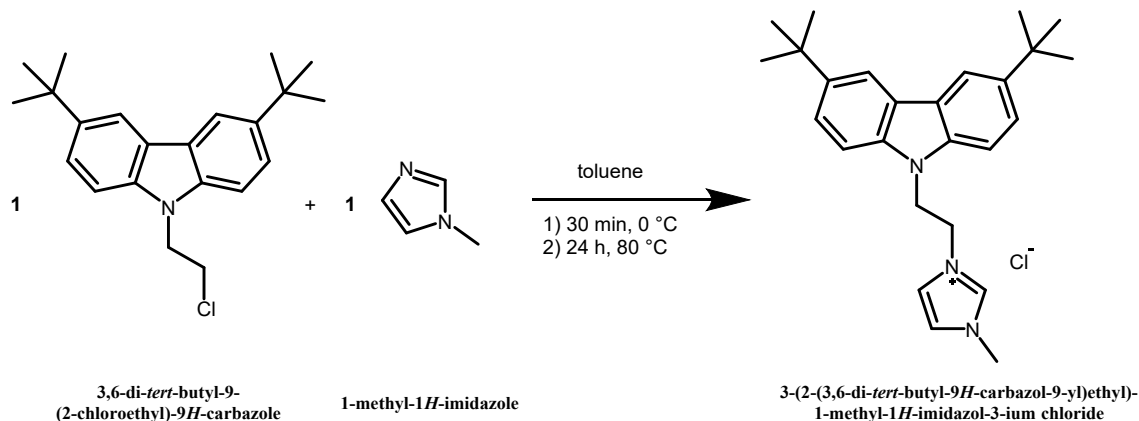**Synthesis of 3,6-di-*tert*-butyl-9-(2-chloroethyl)-9*H*-carbazole**
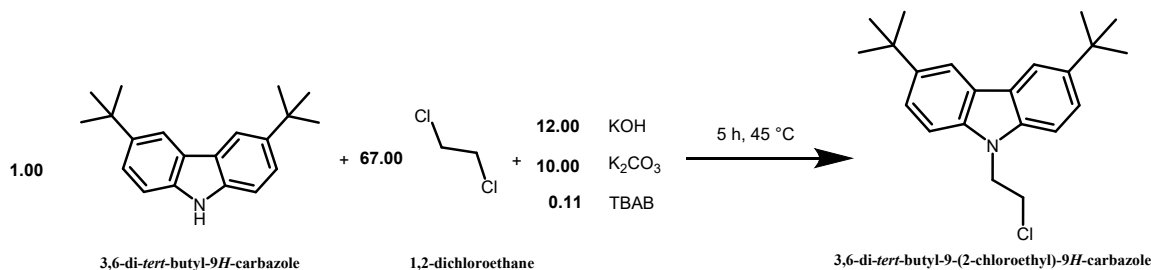
S 5 Synthesis of 3,6-di-*tert*-butyl-9-(2-chloroethyl)-9*H*-carbazole

In a 500 mL round bottom flask equipped with a condenser were loaded 3,6-di-*tert*-butyl-9*H*-carbazole (8.4 g, 0.030 mol), potassium carbonate (20.0 g, 0.15 mol, 10 equiv), potassium hydroxide (8.4 g, 0.18 mol, 12 equiv), tetrabutylammonium bromide (TBAB) (0.5 g, 0.0016 mol, 0.11 equiv) and 1,2-dichloroethane (100 g, 1.01 mol, 67 equiv). The flask was then heated to 50 °C for 5 h subsequently cooled to room temperature and filtered. The solid was then washed with 1,2-dichloroethane (2 x 50 mL). The organic phases were combined, washed with water (2 x 50 mL) and then dried with sodium sulfate. Once the removing the sodium sulfate by filtration, the solvent was removed in the rotary evaporator (40 °C, 200 mbar) producing a white-orange powder. This solid recrystallized two or three times from hot ethanol.

¹H NMR (600 MHz, CDCl₃) δ (ppm) 8.09 (s, 2H), 7.51 (d, *J* = 8.31 Hz, 2H), 7.32 (d, *J* = 8.33 Hz, 2H), 4.57 (t, *J* = 6.8 Hz, 2H), 3.82 (t, *J* = 6.74 Hz, 2H), 1.45 (s, 18H); ¹³C NMR (600 MHz, CDCl₃) δ (ppm) c, 138.7, 123.6, 123.1, 116.5, 107.8, 44.9, 41.1, 34.7, 32.0.

Synthesis of 3-(2-(3,6-di-*tert*-butyl-9*H*-carbazol-9-yl)ethyl)-1-methyl-1*H*-imidazol-3-ium chloride

| 3,6-di-*tert*-butyl-9-(2-chloroethyl)-9*H*-carbazole | 1-methyl-1*H*-imidazole | 3-(2-(3,6-di-*tert*-butyl-9*H*-carbazol-9-yl)ethyl)-1-methyl-1*H*-imidazol-3-ium chloride |

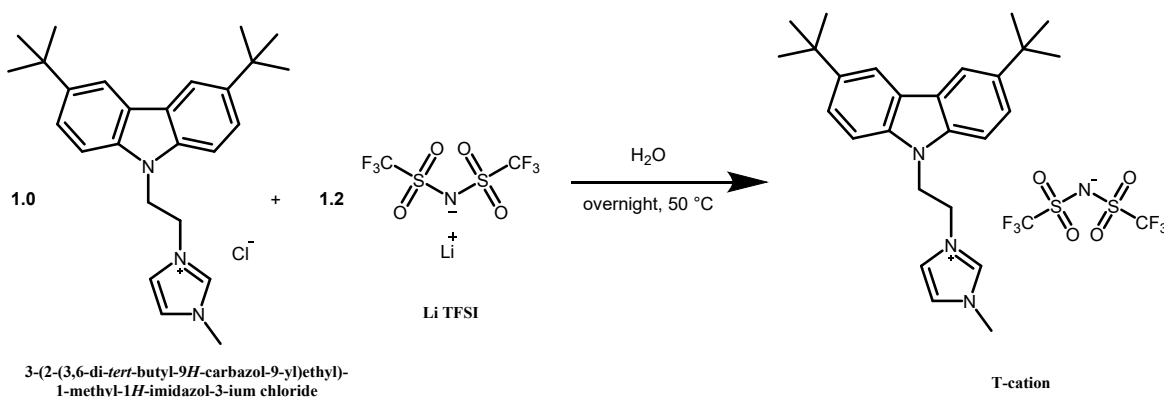**S 6** Synthesis of 3-(2-(3,6-di-*tert*-butyl-9*H*-carbazol-9-yl)ethyl)-1-methyl-1*H*-imidazol-3-ium chloride

All glassware was previously dried prior to reaction. Into a dry two-neck 25 mL round bottom flask equipped with a condenser in the main neck and a silicon septum in the side-neck, were loaded 3,6-di-*tert*-butyl-9-(2-chloroethyl)-9*H*-carbazole (1.3 g, 3.8 mol) and anhydrous DMF (10 mL). Under stirring, three vacuum-argon cycles were then performed to remove residual moisture or atmospheric gases from the reaction mixture. Next, under stirring and argon gas, *N*-methylimidazole (0.31 g, 3.8 mol, 1 equiv) was added to the reaction mixture dropwise over 10 min. After the addition, the reaction mixture was heated to 115 °C for 16 h. The reaction was then cooled to room temperature and approximately half of the DMF was removed under reduced pressure. Ethyl acetate (25 mL) was then added to the solution and a dark orange viscous liquid separated formed. The viscous liquid was then extracted, sonicated in hot ethyl acetate (2 x 25 mL) then washed with CH₂Cl₂ (50 mL).

¹H NMR (600 MHz, DMSO) δ (ppm) 8.84 (s, 1H), 8.19 (s, 2H), 7.72 (s, 1H), 7.60 (s, 1H), 7.44 (d, *J* = 8.5 Hz, 2H), 7.37 (d, *J* = 7.9 Hz, 2H), 4.80 (t, *J* = 5.2 Hz, 2H), 4.59 (t, *J* = 5.4 Hz, 2H), 3.62

(s, 3H), 1.40 (s, 18H); ^{13}C NMR (600 MHz, DMSO) δ (ppm) c, 138.3, 137.0, 123.5, 123.1, 122.9, 122.2, 116.5, 108.1, 47.8, 42.6, 35.4, 34.4

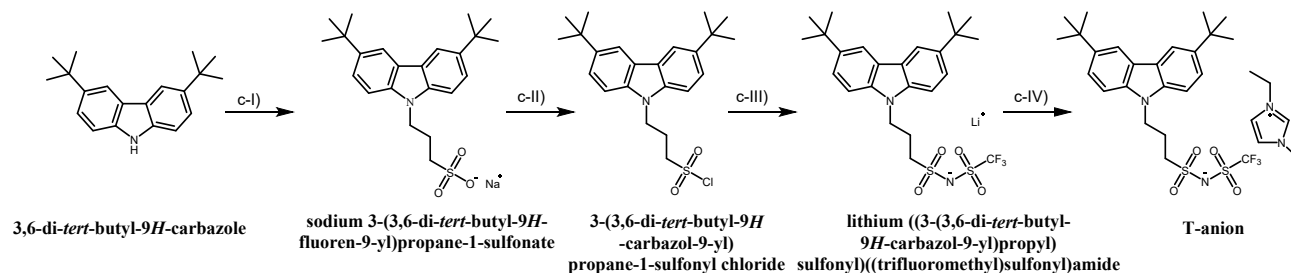**Synthesis of 3-(2-(3,6-di-*tert*-butyl-9*H*-carbazol-9-yl)ethyl)-1-methyl-1*H*-imidazol-3-ium TFSI (*T-cation*)**

3-(2-(3,6-di-*tert*-butyl-9*H*-carbazol-9-yl)ethyl)-
1-methyl-1*H*-imidazol-3-ium chloride

Li TFSI

T-cation

S 7 Synthesis of 3-(2-(3,6-di-*tert*-butyl-9*H*-carbazol-9-yl)ethyl)-1-methyl-1*H*-imidazol-3-ium
TFSI (***T-cation***)

In a 50 mL round bottom flask was added 3-(2-(3,6-di-*tert*-butyl-9*H*-carbazol-9-yl)ethyl)-1-methyl-1*H*-imidazol-3-ium chloride (0.50 g, 1.2 mmol, 1 equiv) and 15 mL of water. This solution was stirred and heated to 50 °C then a solution of Li*TFSI* (0.40 g, 1.4 mmol, 1.2 equiv) in 5 mL of water was added dropwise over a period of 10 min. The resulting mixture was stirred at 50 °C for a further 30 min then left to stir at room temperature for 4 h. The solution was then cooled in an ice-bath and the aqueous phase was removed. The resulting brown-orange viscous liquid was dissolved in CH_2Cl_2 and washed twice with water. The organic phase was then collected and dried to yield the target compound as a golden solid.

^{1}H NMR (600 MHz, DMSO) δ (ppm) 8.66 (s, 1H), 8.19 (s, $^2J_{HH}$ = 1.1, 2H), 7.68 (s, 1H), 7.57 (s, 1H), 7.45 (dd, J = 3.3 Hz, 2H), 7.33 (d, J = 8.6 Hz, 2H), 4.77 (t, J = 5.7 Hz, 2H), 4.60 (t, J = 5.7 Hz, 2H), 3.60 (s, 3H), 1.41 (s, 18H); ^{13}C NMR (600 MHz, DMSO) δ (ppm) c, 138.8, 137.4,124.1, 123.7, 123.4, 122.8, 121.0, 118.9, 117.0, 108.5, 48.4, 43.1, 35.9, 34.9.

Synthesis of 3-ethyl-1-methyl-1*H*-imidazol-3-ium ((3-(3,6-di-tert-butyl-9*H*-carbazol-9-yl)propyl)sulfonyl)((trifluoromethyl)sulfonyl)amide (*T-anion*)

S 8 The overview reaction scheme of synthesis of 3-ethyl-1-methyl-1*H*-imidazol-3-ium ((3-(3,6-di-tert-butyl-9*H*-carbazol-9-yl)propyl)sulfonyl)((trifluoromethyl)sulfonyl)amide (*T-anion*)

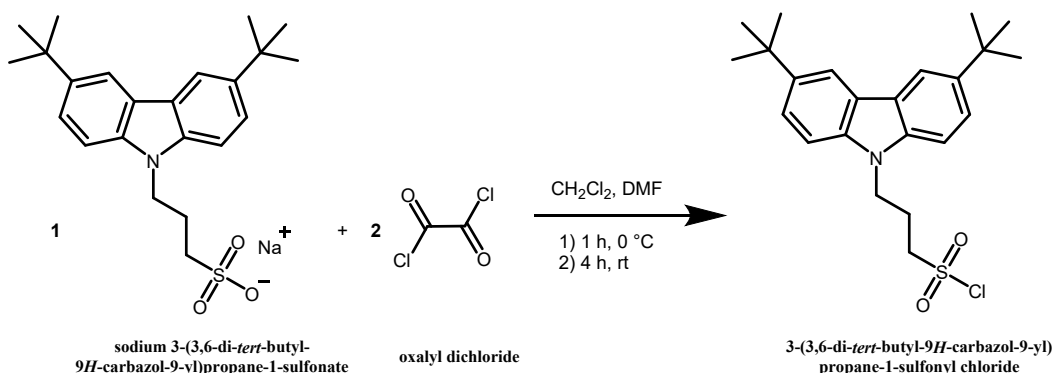**Synthesis of sodium 3-(3,6-di-*tert*-butyl-9*H*-carbazol-9-yl)propane-1-sulfonate**
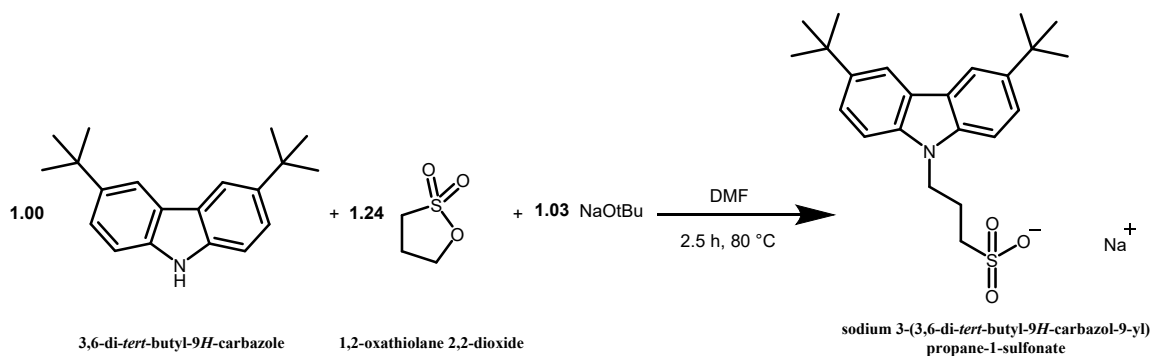
S 9 Synthesis of sodium 3-(3,6-di-*tert*-butyl-9*H*-carbazol-9-yl)propane-1-sulfonate

Dry sodium *t*-butoxide (0.41 g, 4.27 mmol, 1.03 equiv), 3,6-di-*tert*-butyl-9*H*-carbazole (1.16 g, 4.15 mmol, 1.00 equiv) and dry acetonitrile (45 mL) were added into a dried 100 mL two-neck round bottom equipped with a condenser in the main neck and a silicon septum in the side-neck. Under stirring, three vacuum-argon cycles were then performed to remove residual moisture or atmospheric gases from the reaction mixture. Next, 1,3-propane sultone (0.63 g, 5.15 mmol, 1.24 equiv) dissolved in 1 mL of dry acetonitrile was added dropwise over 10 min at room temperature and under Argon atmosphere. The solution was then heated to 80 °C for 5 h producing a white opaque solution. The reaction mixture was then cooled in an ice bath, yielding a white solid which was extracted by filtration, dried *in vacu*o then recrystallized in MeOH/acetonitrile (20/80 vol) to yield the target compound.

^{1}H NMR (600 MHz, DMSO) δ (ppm) 8.16 (s, 2H), 7.50 (quint, $J = 9.7$ Hz, 4H), 4.45 (t, $J = 6.66$ Hz, 2H), 2.37 (t, $J = 6.8$ Hz, 2H), 2.05 (p, $J = 6.9$ Hz, 2H), 1.42 (s, 18H); ^{13}C NMR (600 MHz, DMSO) δ (ppm) 140.8, 138.5, 123.0, 121.9, 116.1, 108.7, 48.7, 41.2, 34.3, 31.9, 25.1

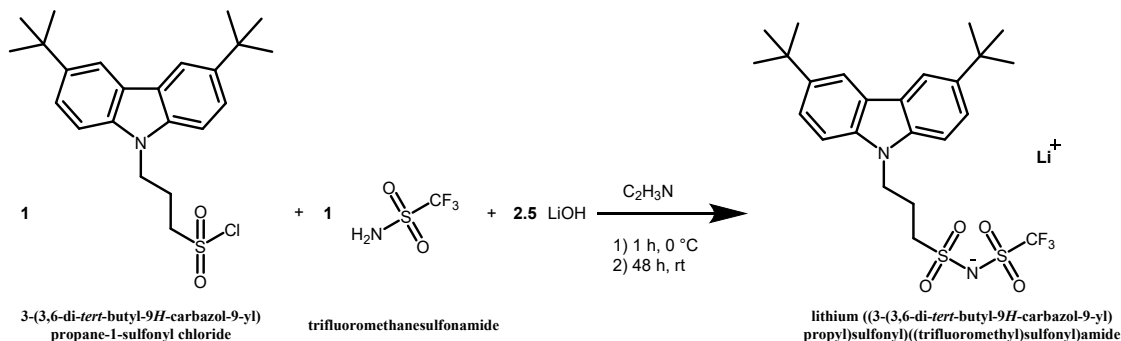**Synthesis of 3-(3,6-di-*tert*-butyl-9*H*-carbazol-9-yl)propane-1-sulfonyl chloride**

S 10 Synthesis of 3-(3,6-di-*tert*-butyl-9*H*-carbazol-9-yl)propane-1-sulfonyl chloride

    In a dry 50 mL two neck round bottom flask equipped with an argon supply on the main neck, a silicon septum on the side neck and a magnetic stirrer were loaded sodium 3-(3,6-di-*tert*-butyl-9*H*-carbazol-9-yl)propane-1-sulfonate (1.0 g, 2.4 mmol ,1 equiv), anhydrous CH_2Cl_2 (8.8 mL) and anhydrous DMF (0.22 mL). This flask was then purged with three vacuum-argon cycles and cooled to 0 °C in an ice bath. Oxalyl chloride (0.66 g, 4.7 mmol, 2 equiv) was then added over the period of 10 min. The reaction was then stirred for 1 h at 0 °C then stirred at room temperate for a further 3 h. The solvents and excess oxalyl chloride were then removed *in vacuo* to yield a yellow-orange solid. The product was used in the next step without further purification.

^{1}H NMR (600 MHz, CDCl$_3$) δ (ppm) 8.12 (s, 2H), 7.53 (d, $J = 8.5$ Hz, 2H), 7.29 (d, $J = 8.5$ Hz, 2H), 4.51 (t, $J = 6.5$ Hz, 2H), 3.63 (t, $J = 7.3$ Hz, 2H), 2.63 (p, $J = 6.8$ Hz, 2H), 1.46 (s, 25H); ^{13}C NMR (600 MHz, CDCl$_3$) δ (ppm) 142.7, 138.7, 124.0, 123.3, 116.8, 107.7, 62.9, 40.6, 34.8, 32.1, 24.4.
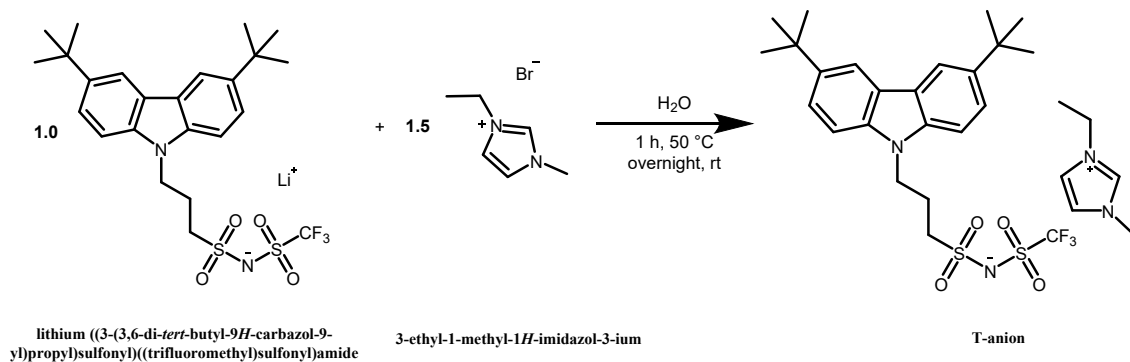
Synthesis of Lithium ((3-(3,6-di-*tert*-butyl-9H-carbazol-9-yl) propyl)sulfonyl) ((trifluoromethyl)sulfonyl)amide

S 11 Synthesis of Lithium ((3-(3,6-di-*tert*-butyl-9*H*-carbazol-9-yl) propyl)sulfonyl) ((trifluoromethyl)sulfonyl)amide

Into a dry 50 mL round bottom flask equipped with magnetic stir bar were loaded trifluoromethanesulfonamide (0.26 g, 1.7 mmol, 1 equiv), dry LiOH (0.11 g, 4.3 mmol, 2.5 equiv) and 5 mL of dry acetonitrile. This mixture was then stirred in an ice bath and purged with N_2. 3-(3,6-di-*tert*-butyl-9*H*-carbazol-9-yl)propane-1-sulfonyl chloride (0.98 g, 3.2 mmol, 1 equiv) dissolved in a minimal amount of dry acetonitrile was then added dropwise to the mixture. The reaction was then left to react for 48 h at room temperature. The resulting white slurry was filtered, and the white solid was washed with ethylacetate 100 mL. The organic phases were combined, filtered again to remove white solids then the solvents were evaporated in vacuo to yield solids. Purification by column chromatography (100% EtOAc) followed by solvent removal yields the pure target compound.

Synthesis of 3-ethyl-1-methyl-1*H*-imidazol-3-ium ((3-(3,6-di-*tert*-butyl-9*H*-carbazol-9-yl)propyl)sulfonyl)((trifluoromethyl)sulfonyl)amide (*T-anion*)


lithium ((3-(3,6-di-*tert*-butyl-9*H*-carbazol-9-yl)propyl)sulfonyl)((trifluoromethyl)sulfonyl)amide

3-ethyl-1-methyl-1*H*-imidazol-3-ium

T-anion

S 12 Synthesis of 3-ethyl-1-methyl-1*H*-imidazol-3-ium ((3-(3,6-di-*tert*-butyl-9*H*-carbazol-9-yl)propyl)sulfonyl)((trifluoromethyl)sulfonyl)amide (***T-anion***)

In a 50 mL round bottom flask equipped with a stir bar was added lithium ((3-(3,6-di-*tert*-butyl-9*H*-carbazol-9-yl)propyl)sulfonyl)((trifluoromethyl)sulfonyl)amide (0.21 g, 0.42 mmol, 1 equiv) and deionized water (25 mL). This was stirred, heated to 50 °C and 3-ethyl-1-methyl-1*H*-imidazol-3-ium bromide (0.12 g, 0.63 mmol, 1.5 equiv) dissolved in deionized water (5 mL) was added dropwise. The reaction was then stirred for 1 h at 50 °C then overnight at room temperature. The resulting reaction mixture was composed of a transparent aqueous phase and a white solid. The water phase was removed then the white solid was sonicated in water (3 x 50 mL) and the aqueous phase was binned. The product was dried in vacuo to yield the target compound as a white solid.

^{1}H NMR (600 MHz, DMSO) δ (ppm) 9.09 (s, 1H), 8.17 (s, 2H), 7.76 (s, 1H), 7.68 (s, 1H), 7.50 (s, 4H), 4.47 (s, 2H), 4.18 (s, $^2J_{HH}$ = 4.9 Hz, 2H), 3.84 (s, 3H), 3.00 (s, 2H), 2.14 (s, 2H), 1.41 (s, 22H); ^{13}C NMR (600 MHz, DMSO) δ (ppm) c, 138.9, 137.1, 123.7, 123.2, 122.9, 121.3, 116.3, 108.4, 52.7, 45.3, 34.8, 24.1, 15.2.

Synthesis of 3,6-di-*tert*-butyl-9-ethyl-9*H*-carbazole (**T-standard**)
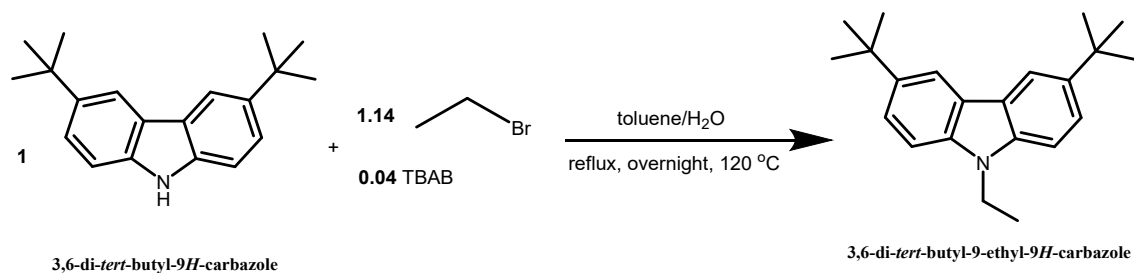

S 13 Synthesis of 3,6-di-*tert*-butyl-9-ethyl-9*H*-carbazole (**T-standard**)

The procedure was adapted from Ameen et al [5]. Into a round-bottom flask, 3,6-di-*tert*-butyl-9*H*-carbazole (1.23 g, 4.39 mmol), tetrabutylammonium bromide (TBAB) (0.05 g, 0.15 mmol, 0.04 equiv), toluene (40 mL) and a 50% sodium hydroxide solution 25 mL were added and vigorously stirred. Bromoethane (0.37 mL, 5.01 mmol, 1.14 equiv) was then added dropwise and left to reflux at 120 °C for 16 h. Once cooled, the organic phase was extracted with CH_2Cl_2 (3 x 50 mL), dried with Na_2SO_4 and the solvent evaporated under reduced pressure to yield a yellow solid. This was then recrystallized twice in the mixture of $EtOH/CH_2Cl_2$ to yield the crystal pellets.

^1H NMR (600 MHz, CDCl$_3$) δ (ppm) 8.11 (s, $^2J_{HH}$ = 1.5, 2H), 7.51 (dd, *Jdoublet* = 1.8, J = 8.5 Hz, 2H), 7.31 (d, J = 8.5 Hz, 2H), 4.32 (q, J = 7.2 Hz, 2H), 1.46 (s, 18H), 1.42 (t, J = 7.2 Hz, 3H); ^{13}C NMR (600 MHz, CDCl$_3$) δ (ppm) 141.6, 138.6, 123.3, 123.0, 116.5, 107.9, 37.7, 34.8, 32.2, 14.1

Supporting data

Nuclear magnetic resonance (NMR) spectra
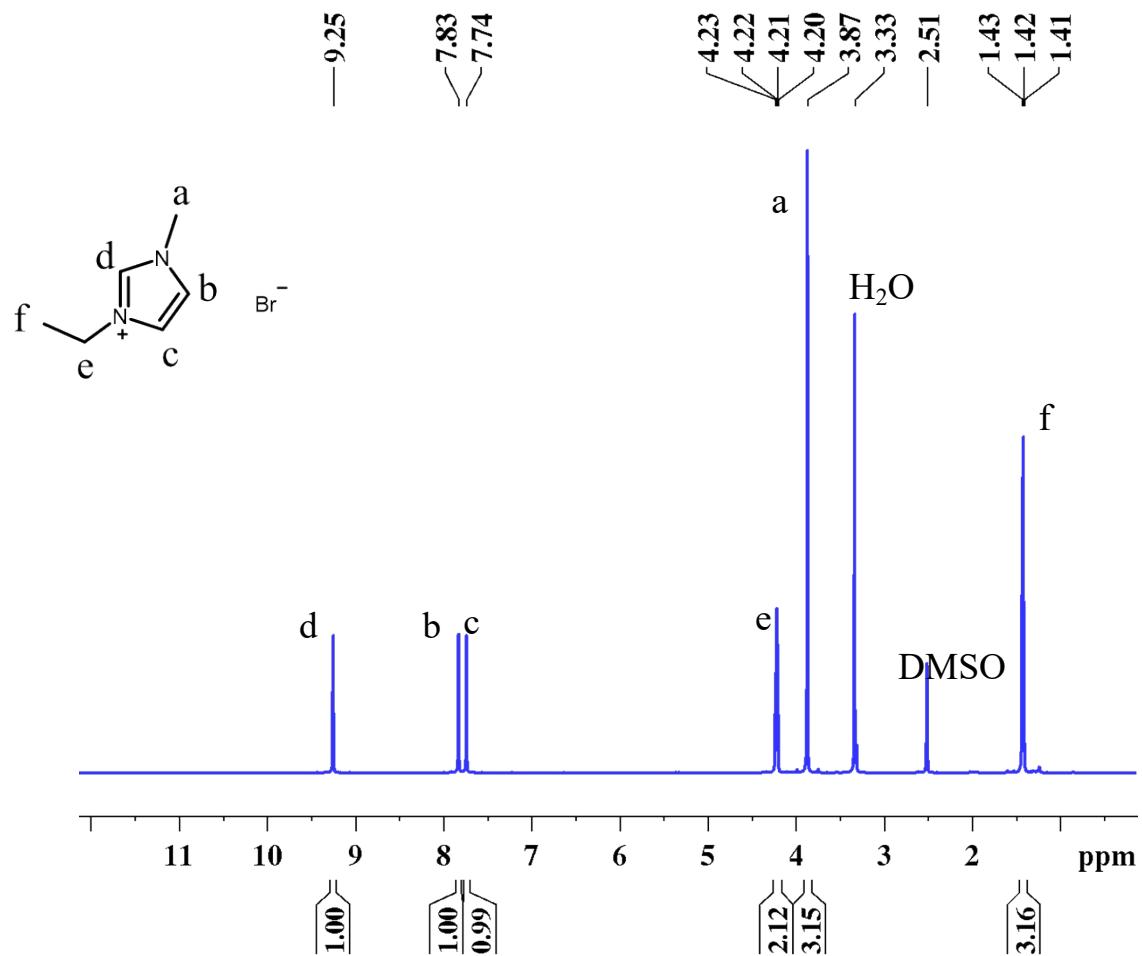
Figure 1 ^{1}H NMR spectra of 3-ethyl-1-methyl-1H-imidazol-3-ium bromide in DMSO-d6
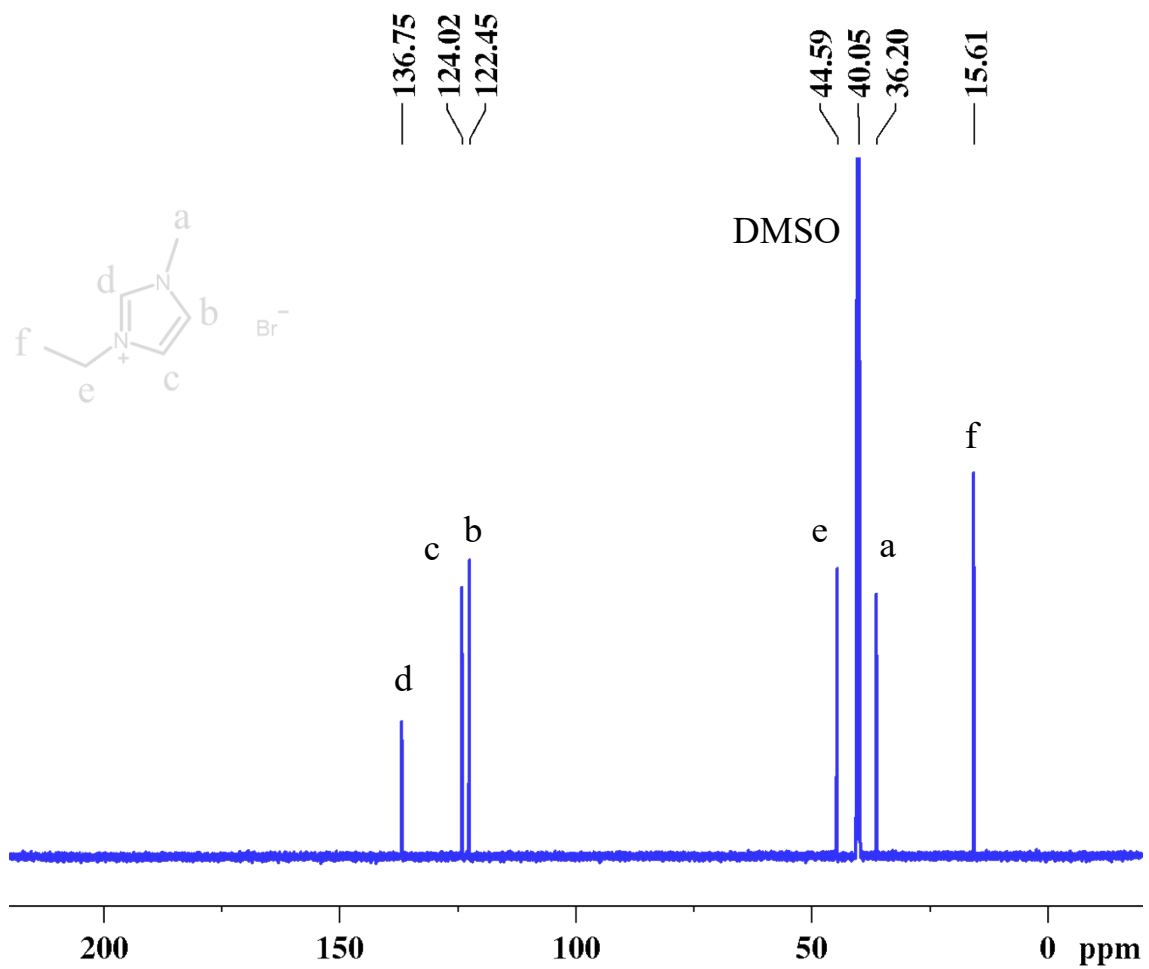
Figure 2 ^{13}C NMR spectra of 3-ethyl-1-methyl-1H-imidazol-3-ium bromide in DMSO-d6

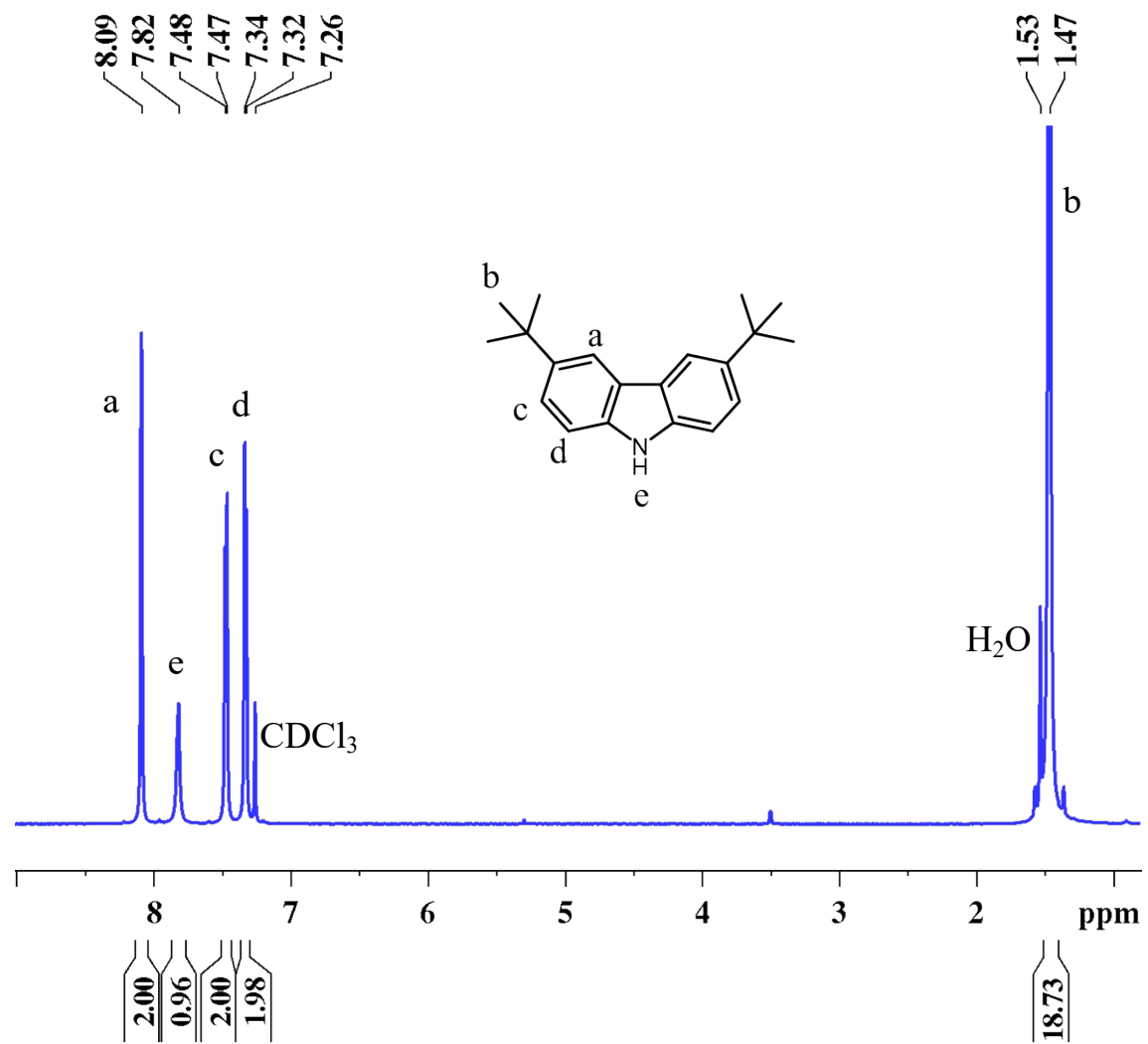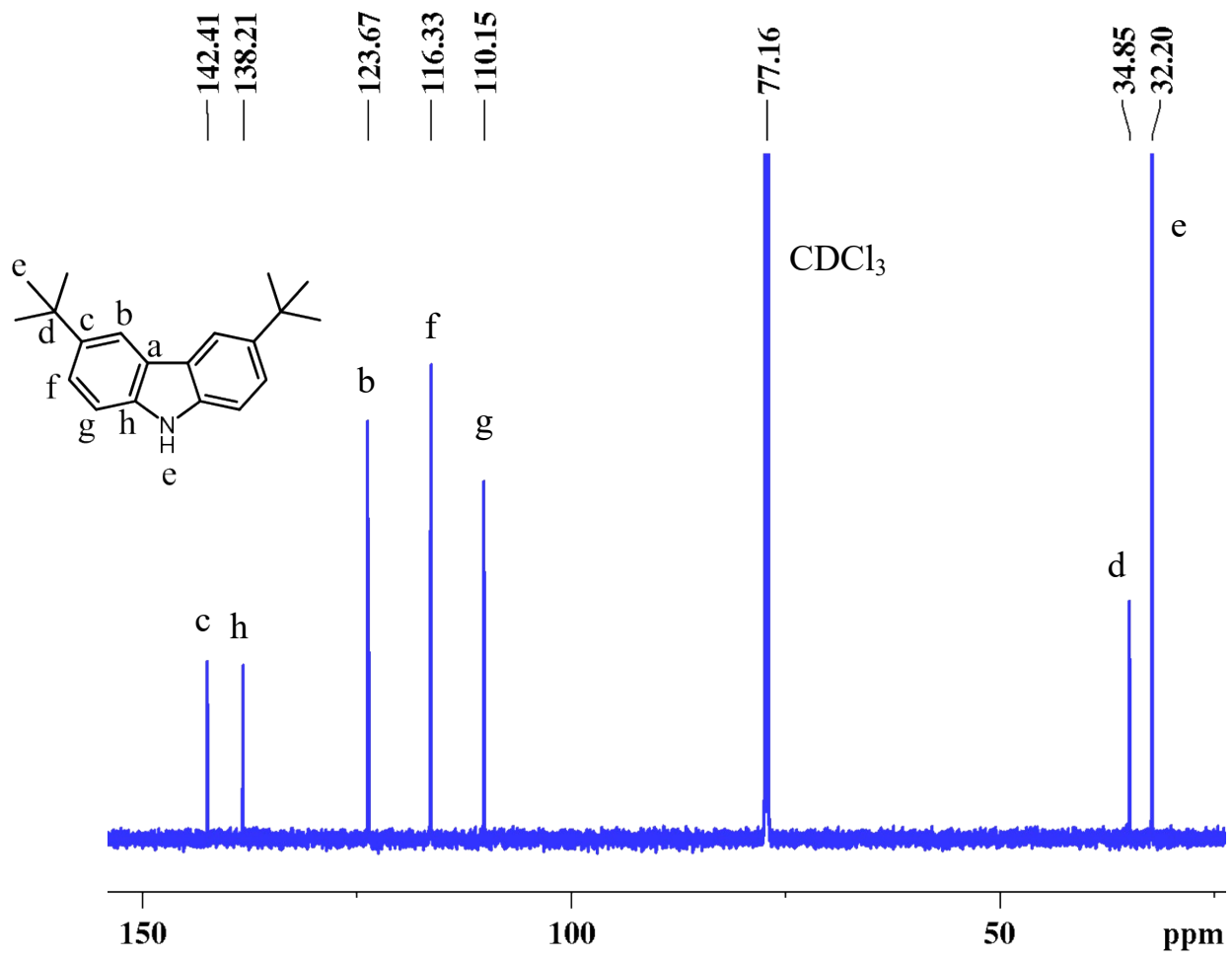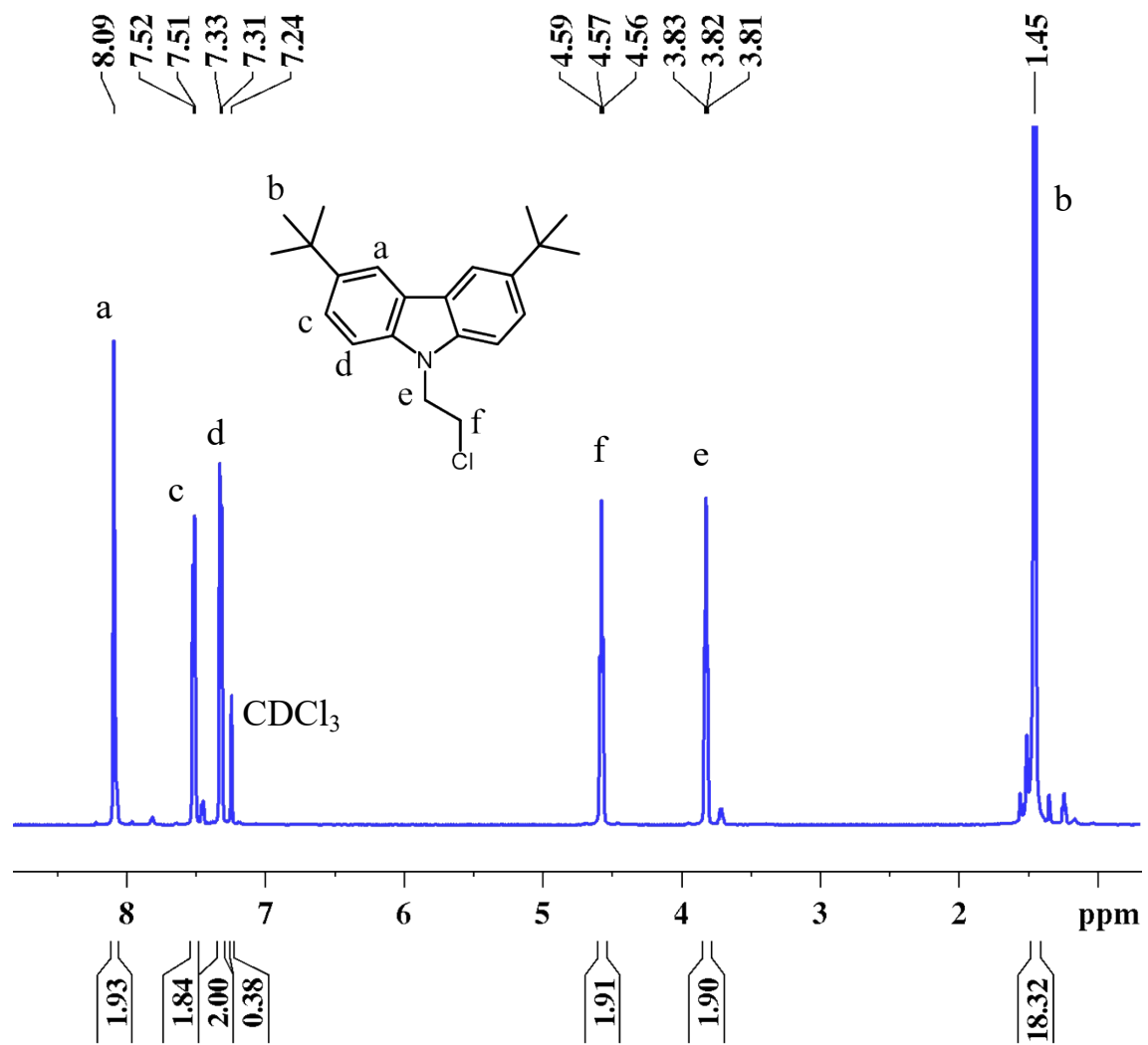**Figure 3** ^{1}H NMR of 3,6-di-*tert*-butyl-9*H*-carbazole in CDCl$_3$

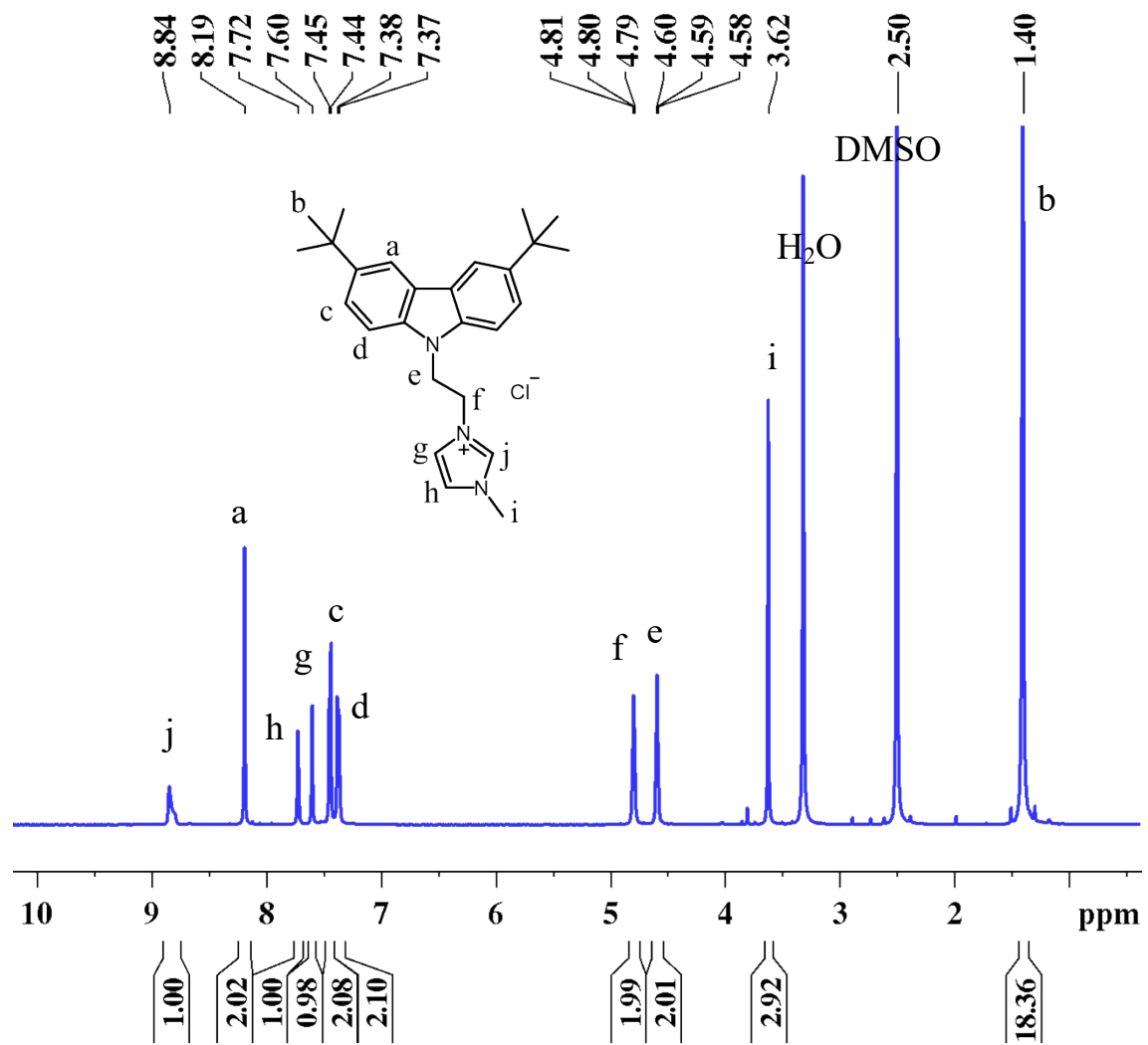**Figure 4** ^{13}C NMR spectra of 3,6-di-*tert*-butyl-9*H*-carbazole in CDCl$_3$

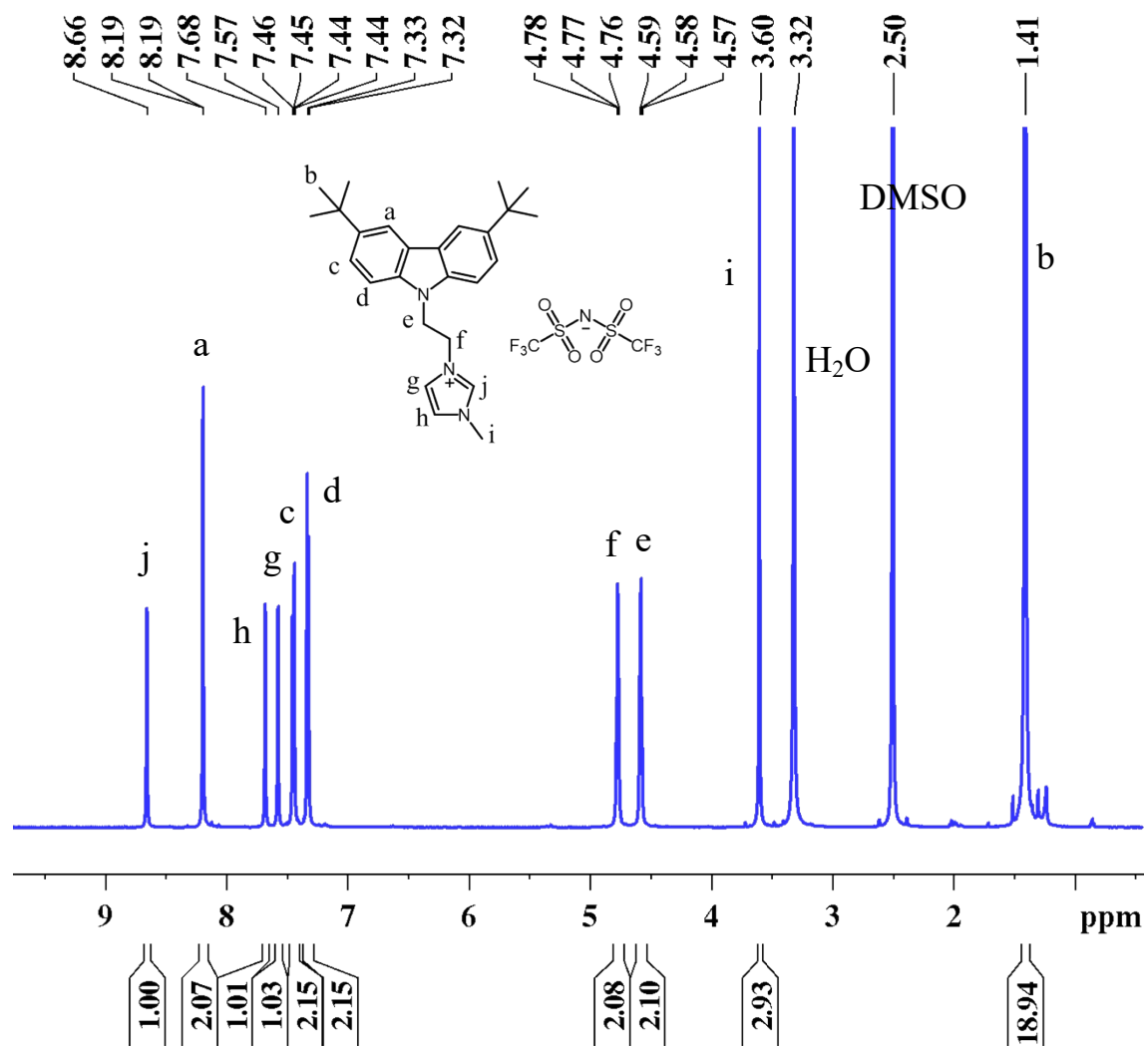**Figure 5** ^{1}H NMR spectra of 3,6-di-*tert*-butyl-9-(2-chloroethyl)-9*H*-carbazole in CDCl$_3$
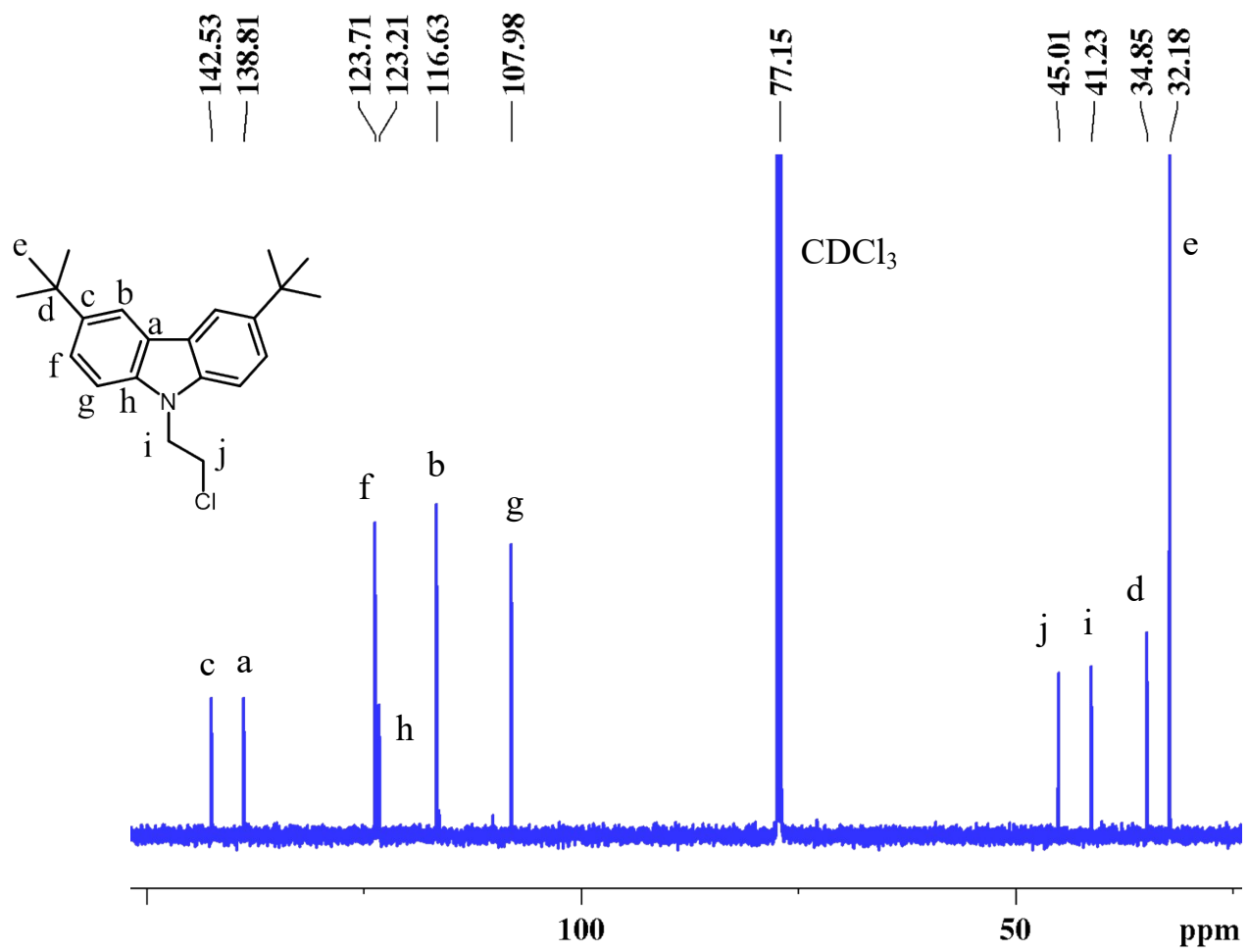
Figure 6 ^{13}C NMR spectra of 3,6-di-*tert*-butyl-9-(2-chloroethyl)-9*H*-carbazole in CDCl$_3$

Figure 7 ^{1}H NMR spectra of 3-(2-(3,6-di-*tert*-butyl-9*H*-carbazol-9-yl)ethyl)-1-methyl-1*H*-imidazol-3-ium chloride in DMSO-d6
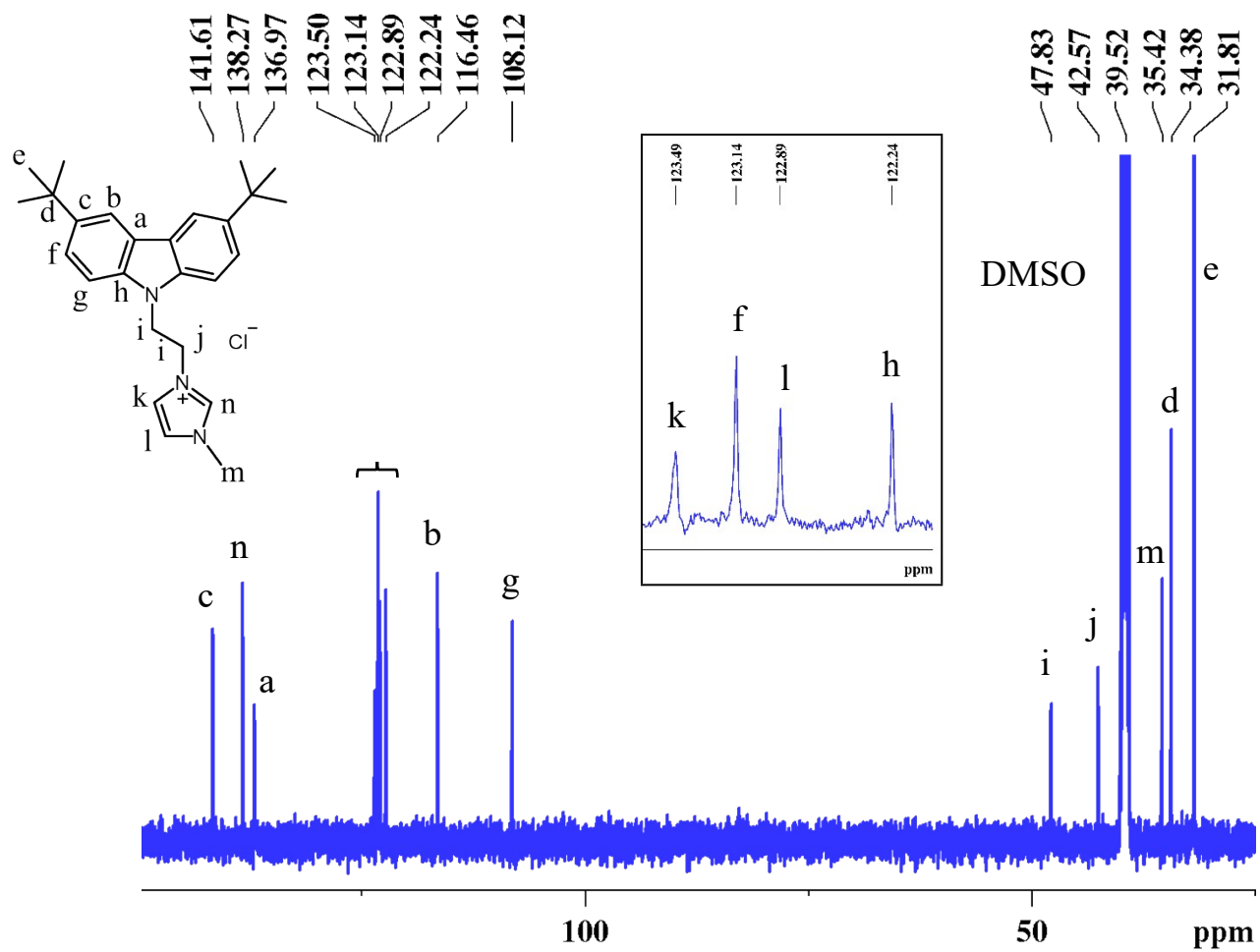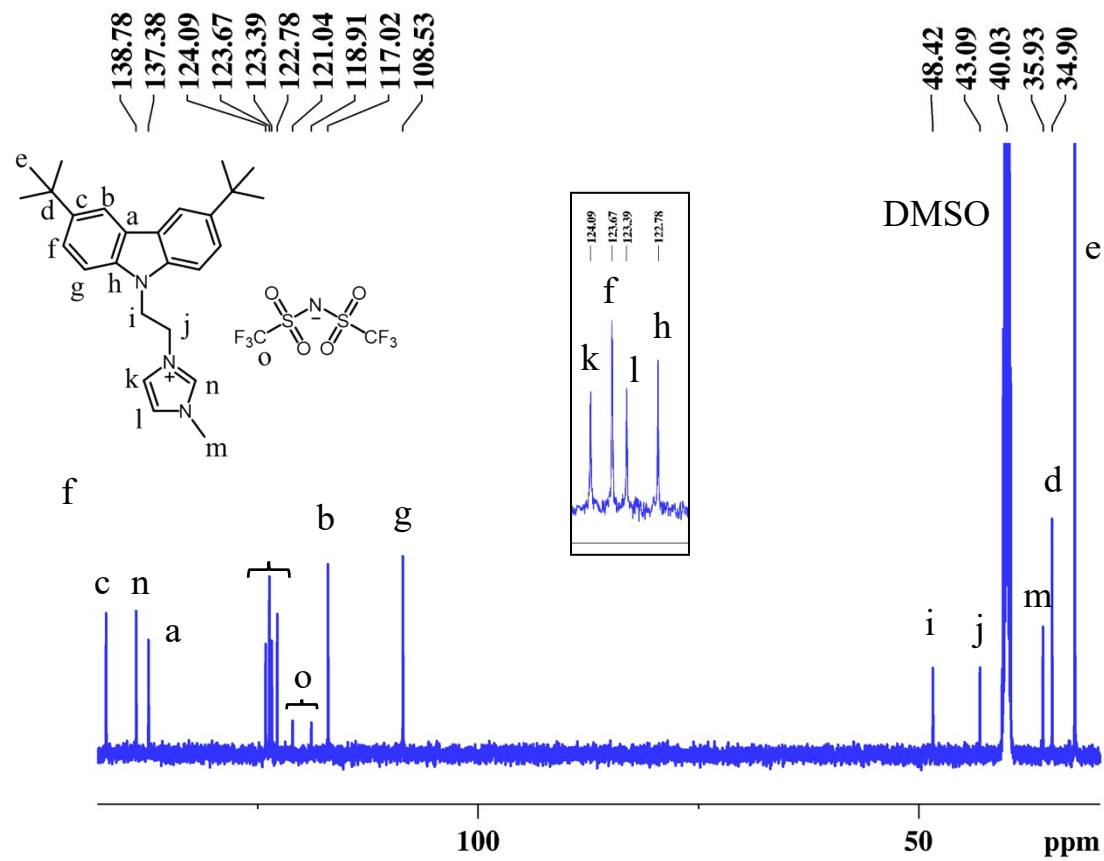
Figure 8 ^{13}C NMR spectra of 3-(2-(3,6-di-*tert*-butyl-9*H*-carbazol-9-yl)ethyl)-1-methyl-1*H*-imidazol-3-ium chloride in DMSO-d6
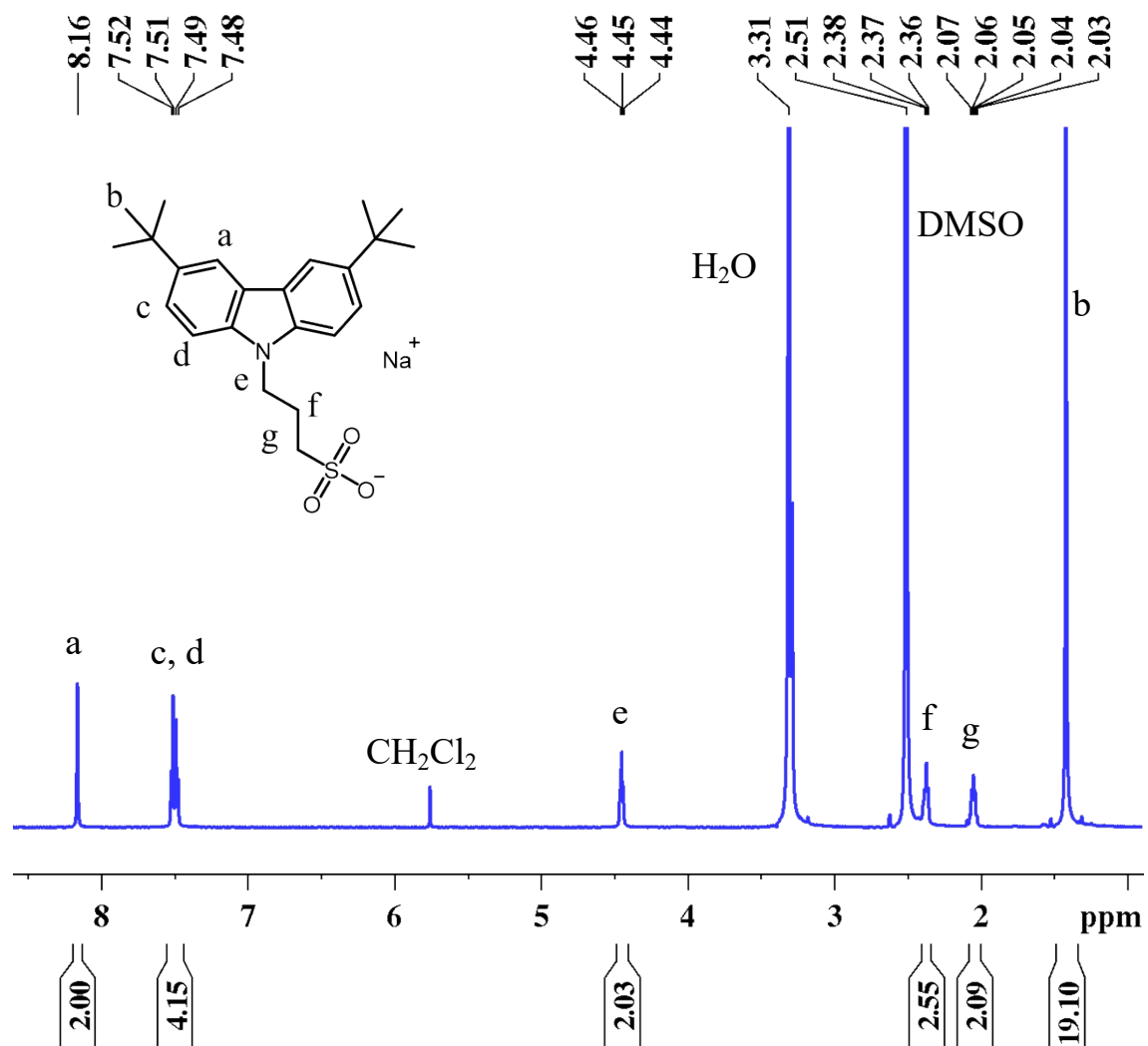
Figure 9 ^{1}H NMR spectra of 3-(2-(3,6-di-*tert*-butyl-9*H*-carbazol-9-yl)ethyl)-1-methyl-1*H*-imidazol-3-ium *TFSI (**T-cation**)* in DMSO-d6
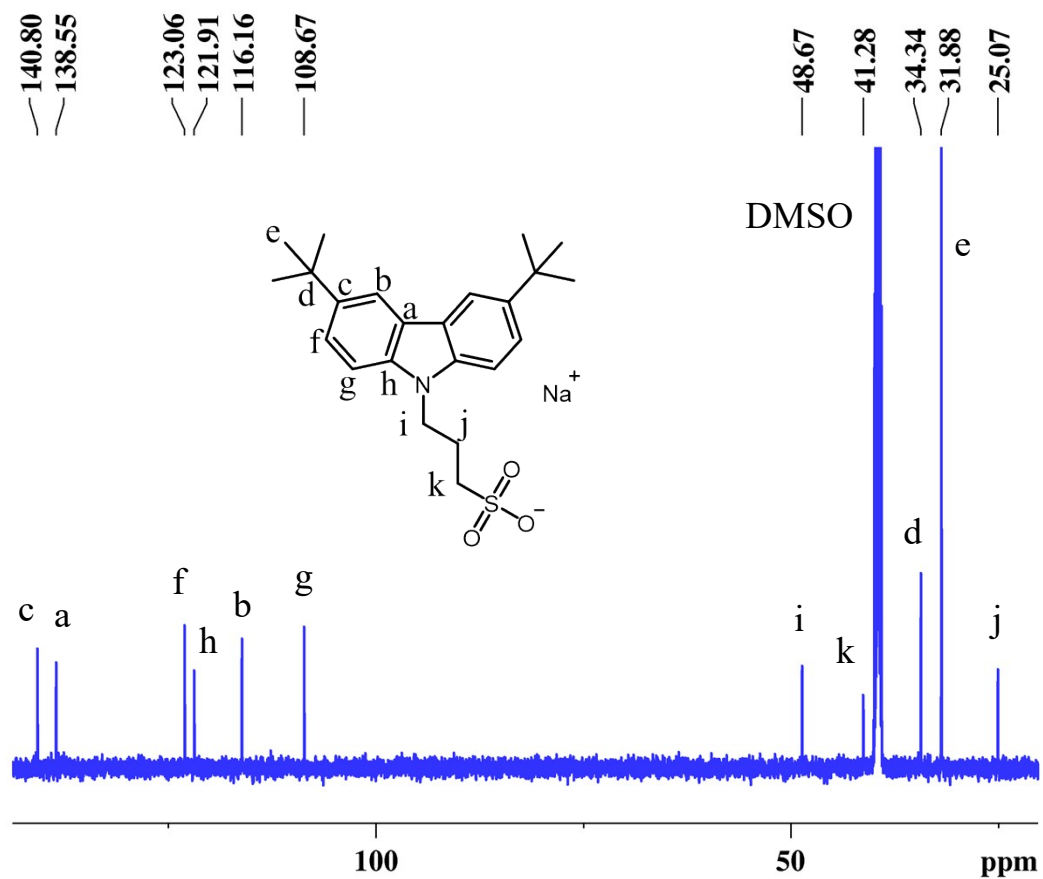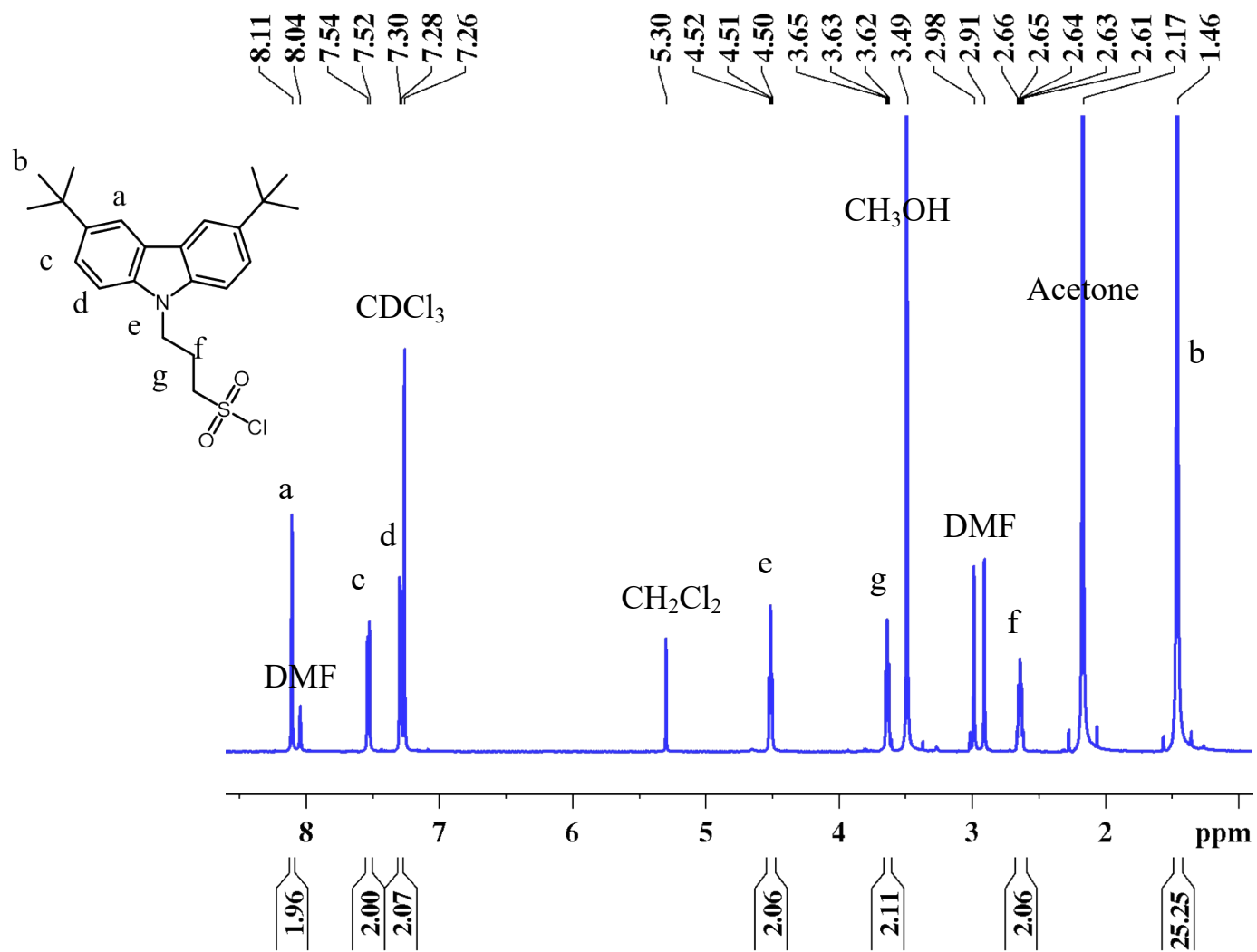
Figure 10 ^{13}C NMR spectra of 3-(2-(3,6-di-*tert*-butyl-9*H*-carbazol-9-yl)ethyl)-1-methyl-1*H*-imidazol-3-ium *TFSI (**T-cation**)* in DMSO-d6
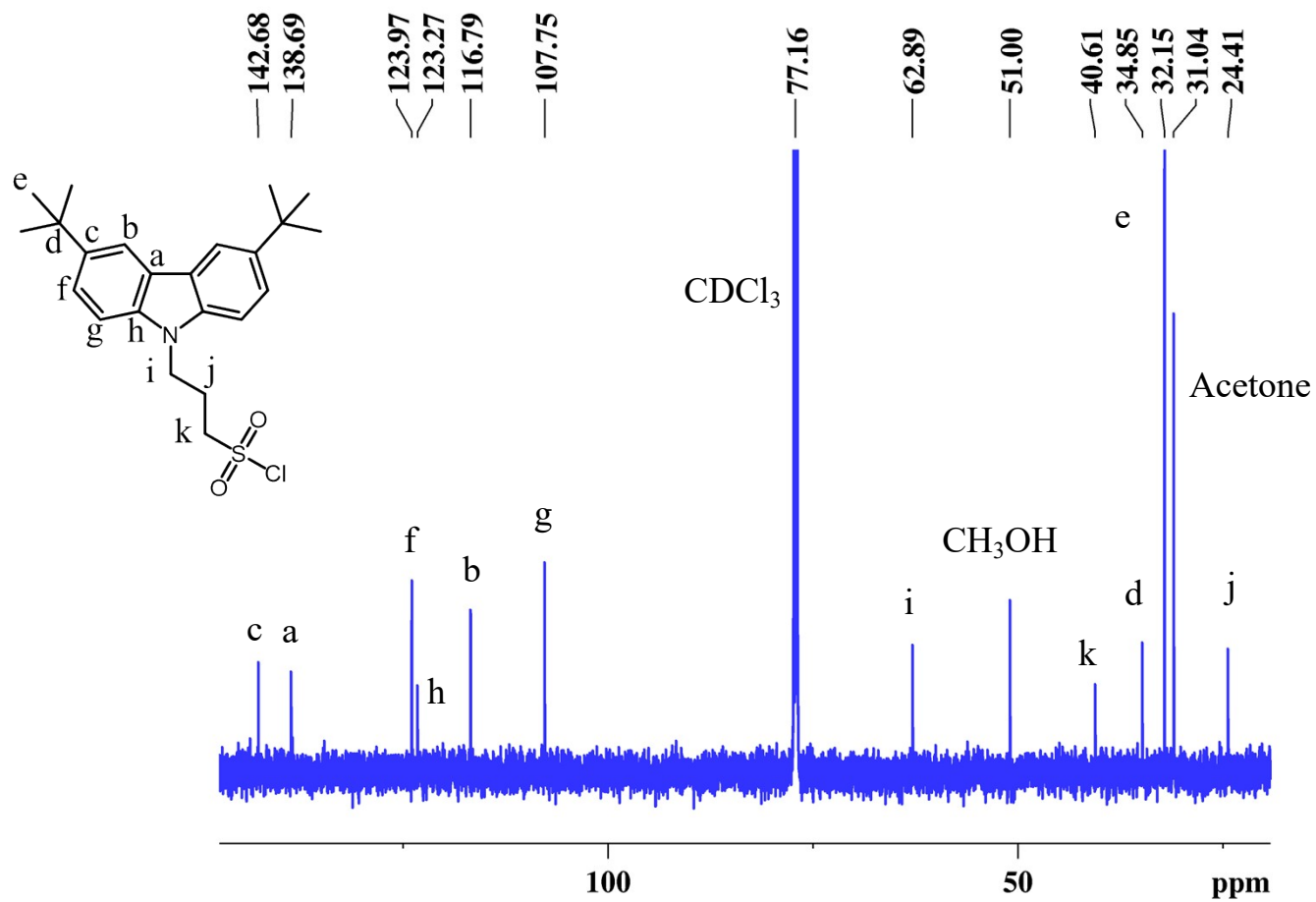
Figure 11 ^{1}H NMR spectra of 3-(3,6-di-*tert*-butyl-9*H*-carbazol-9-yl)propane-1-sulfonate in DMSO-d6

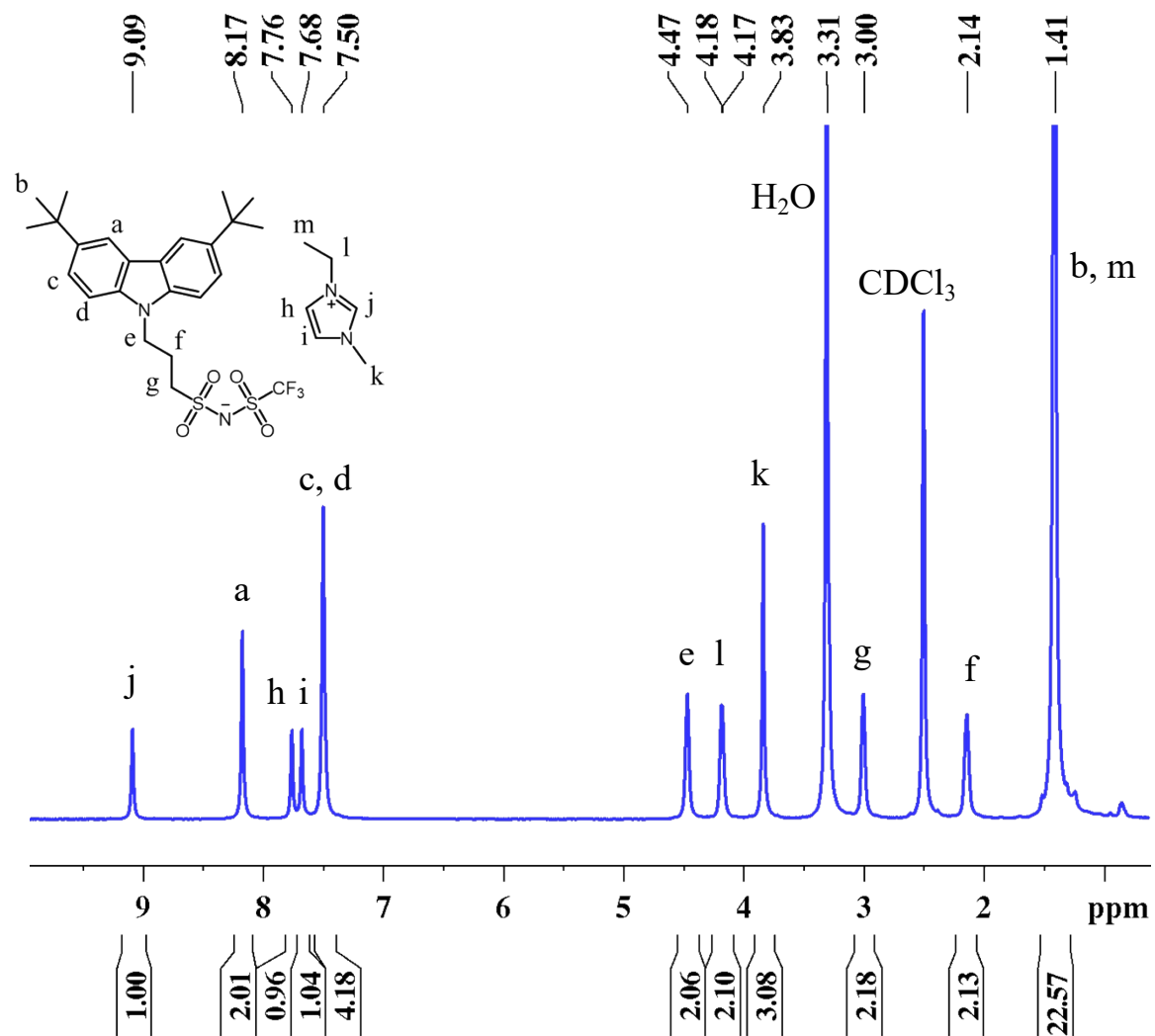**Figure 12** ^{13}C NMR spectra of 3-(3,6-di-*tert*-butyl-9*H*-carbazol-9-yl)propane-1-sulfonate in DMSO-d6

Figure 13 ^{1}H NMR spectra of 3-(3,6-di-*tert*-butyl-9*H*-carbazol-9-yl)propane-1-sulfonyl chloride in CDCl$_3$
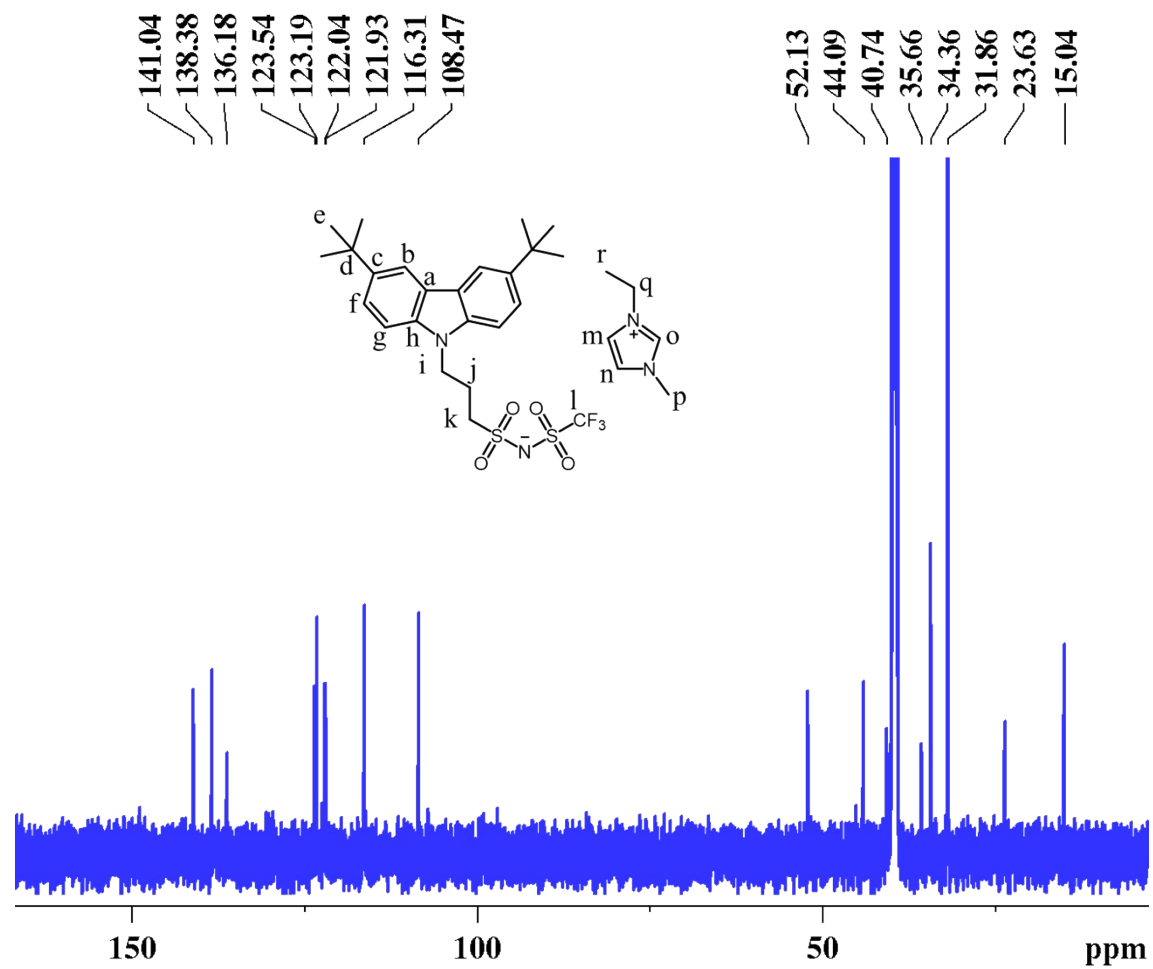
Figure 14 ^{13}C NMR spectra of 3-(3,6-di-*tert*-butyl-9*H*-carbazol-9-yl)propane-1-sulfonyl chloride in CDCl$_3$

Figure 15 ^{1}H NMR spectra of 3-ethyl-1-methyl-1*H*-imidazol-3-ium ((3-(3,6-di-*tert*-butyl-9*H*-carbazol-9-yl)propyl)sulfonyl)((trifluoromethyl)sulfonyl)amide (***T-anion***) in CDCl$_3$

Figure 16 ^{13}C NMR spectra of 3-ethyl-1-methyl-1*H*-imidazol-3-ium ((3-(3,6-di-*tert*-butyl-9*H*-carbazol-9-yl)propyl)sulfonyl)((trifluoromethyl)sulfonyl)amide (***T-anion***) in CDCl$_3$
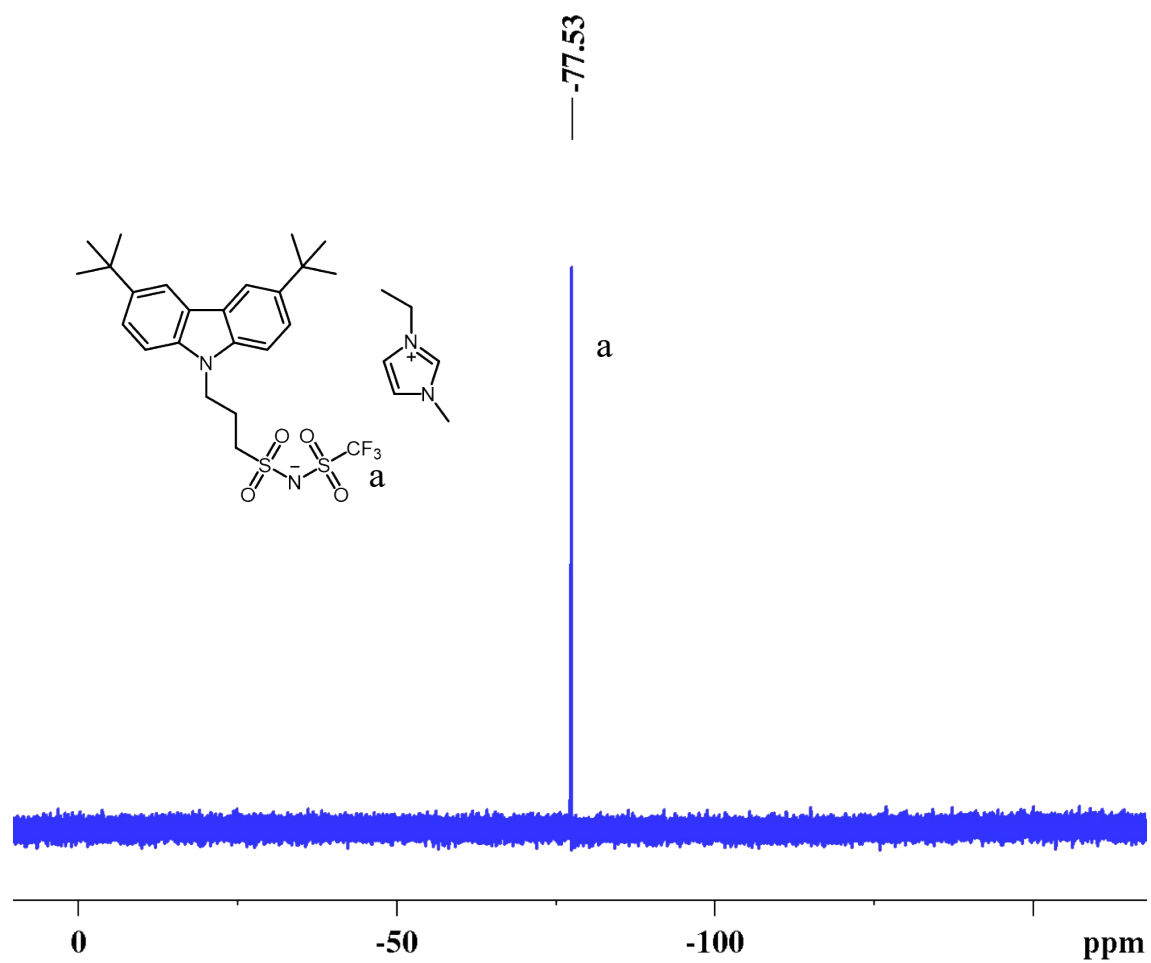
Figure 17 ^{19}F NMR spectra of 3-ethyl-1-methyl-1*H*-imidazol-3-ium ((3-(3,6-di-*tert*-butyl-9*H*-carbazol-9-yl)propyl)sulfonyl)((trifluoromethyl)sulfonyl)amide (***T-anion***) in CDCl$_3$
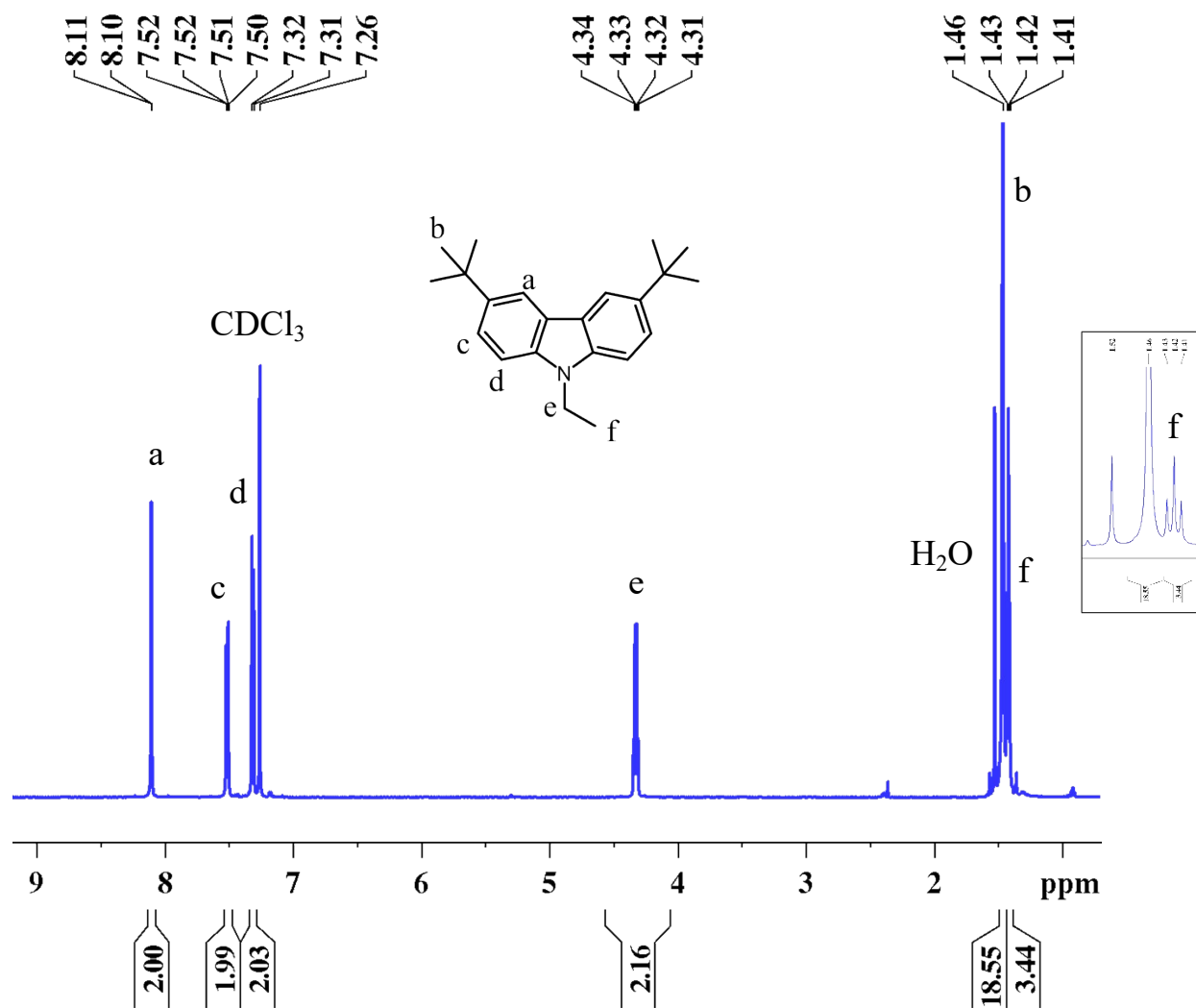
Figure 18 ^{1}H NMR spectra of 3,6-di-*tert*-butyl-9-ethyl-9*H*-carbazole in CDCl$_3$
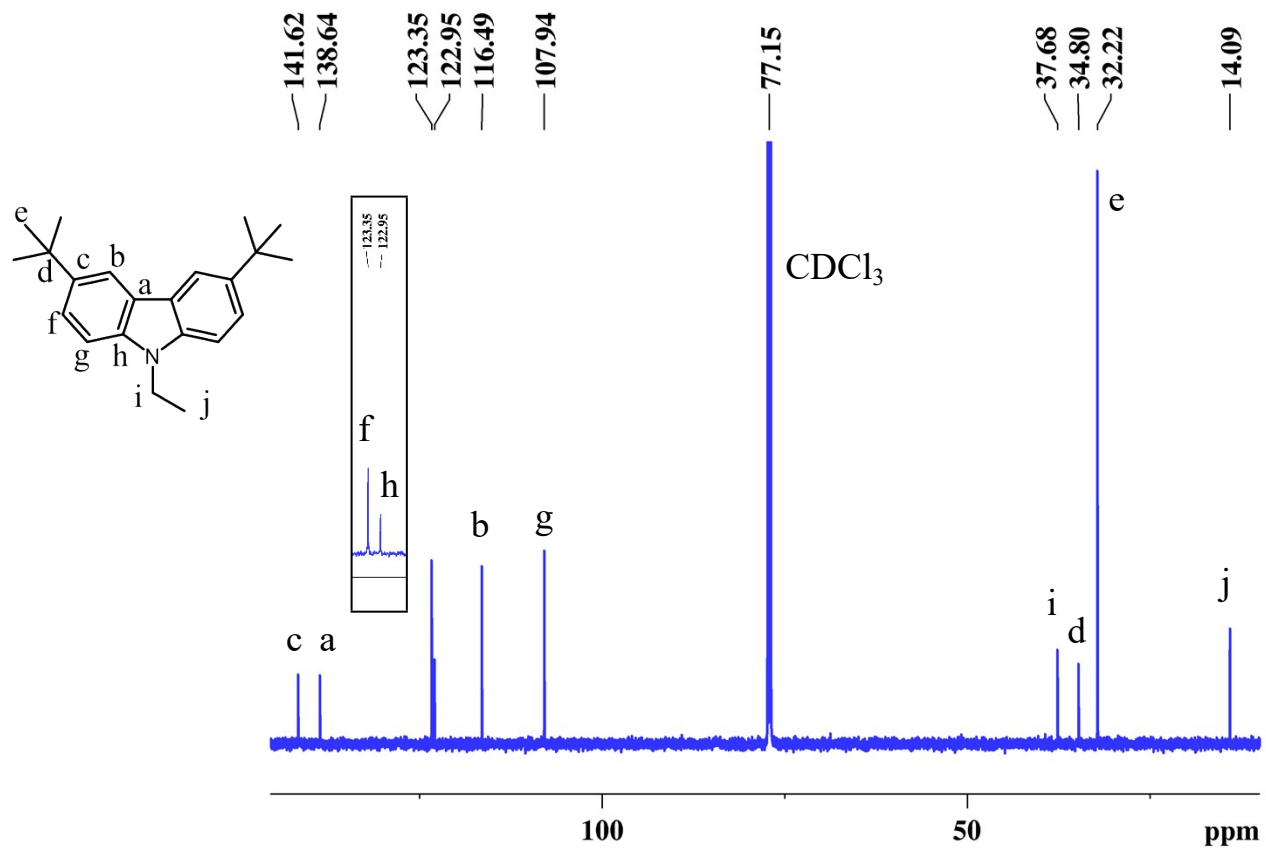
Figure 19 ^{13}C NMR spectra of 3,6-di-*tert*-butyl-9-ethyl-9*H*-carbazole in CDCl$_3$

Fourier-transform infrared (FT-IR)
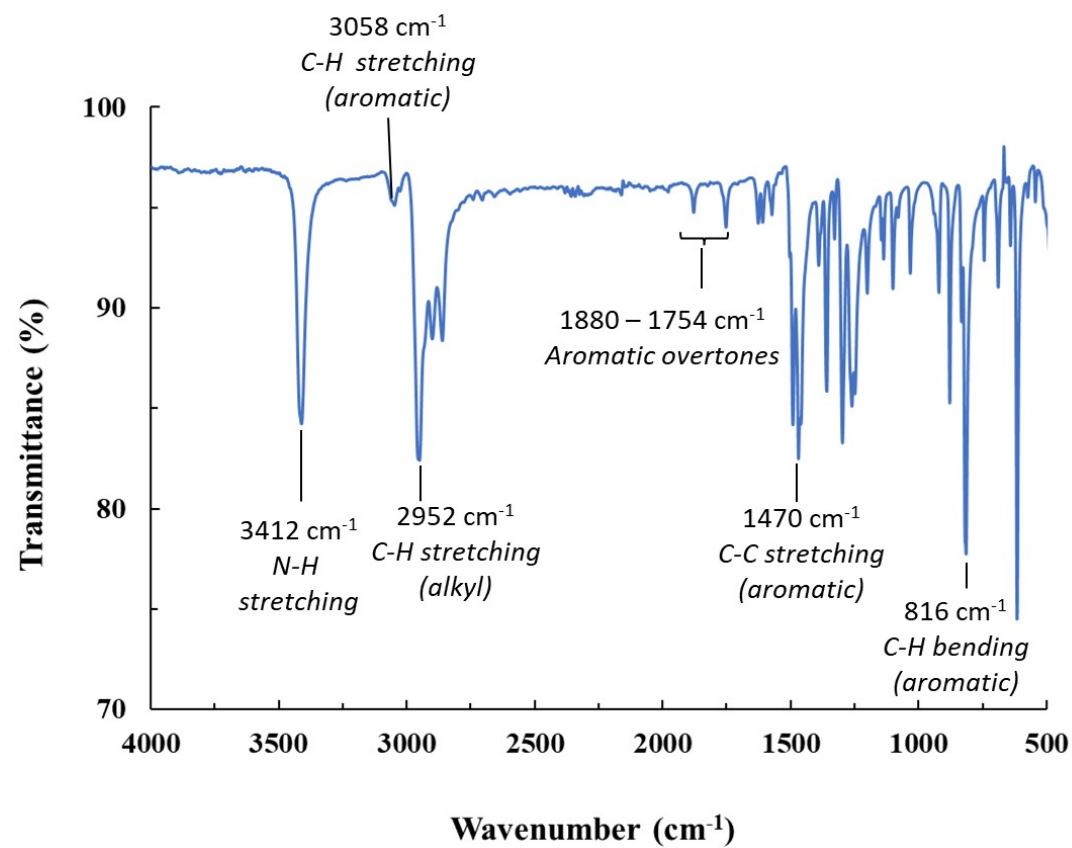
3412; 3058; 2952; 1880–1754; 1470; 816 cm^{-1}

Figure 20 FTIR spectra of 3,6-di-*tert*-butyl-9*H*-carbazole
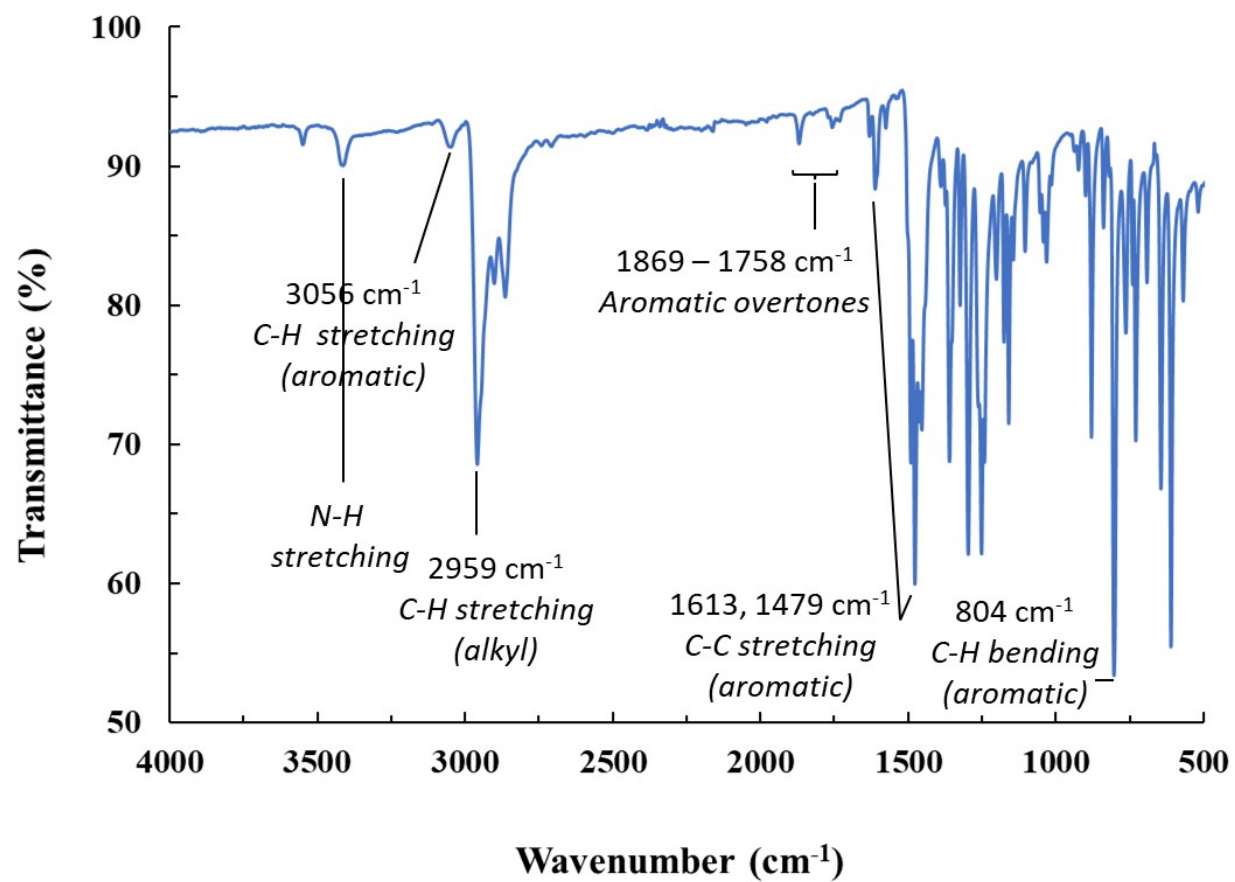
$$3056; 2959; 1869–1758; 1613; 1479; 804 \text{ cm}^{-1}$$

Figure 21 FTIR spectra of 3,6-di-*tert*-butyl-9-(2-chloroethyl)-9*H*-carbazole
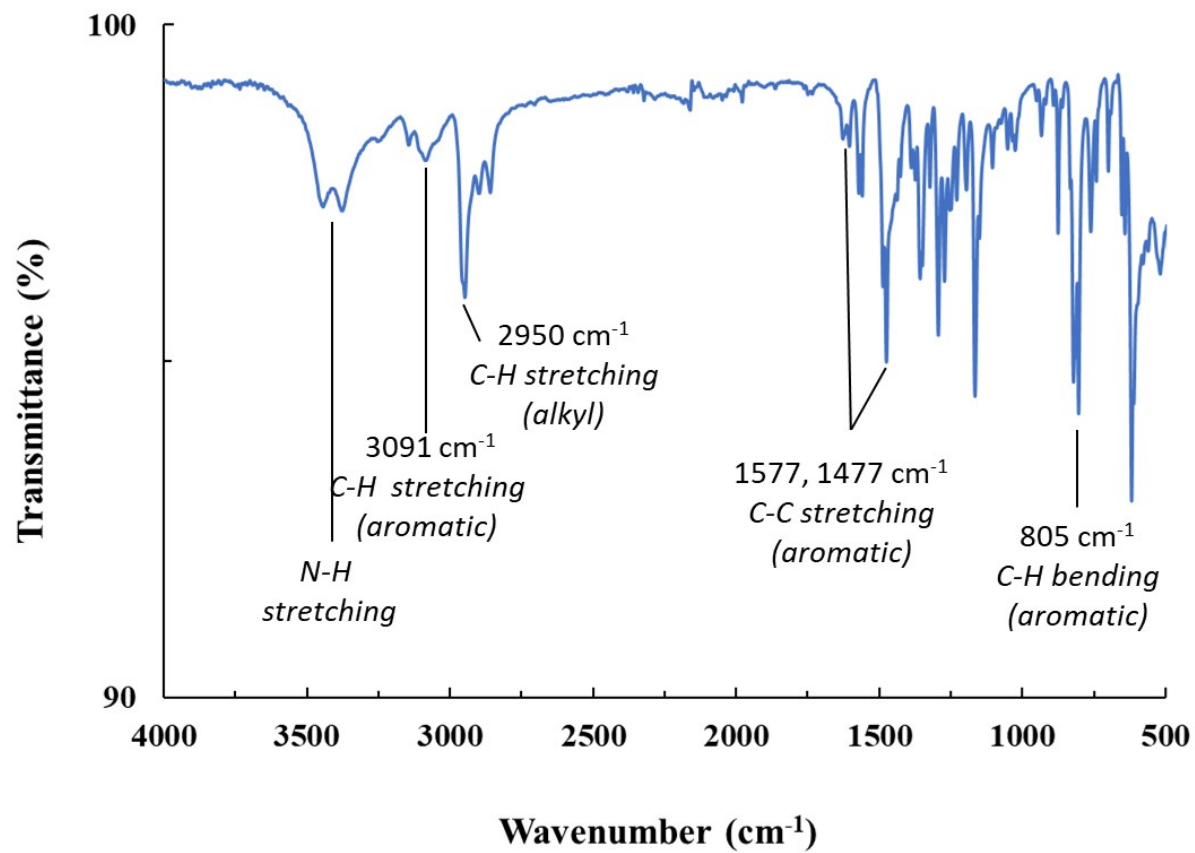
3091; 2950; 1577; 1477; 805 cm^{-1}

Figure 22 FTIR spectra of 3-(2-(3,6-di-*tert*-butyl-9*H*-carbazol-9-yl)ethyl)-1-methyl-1*H*-imidazol-3-ium chloride
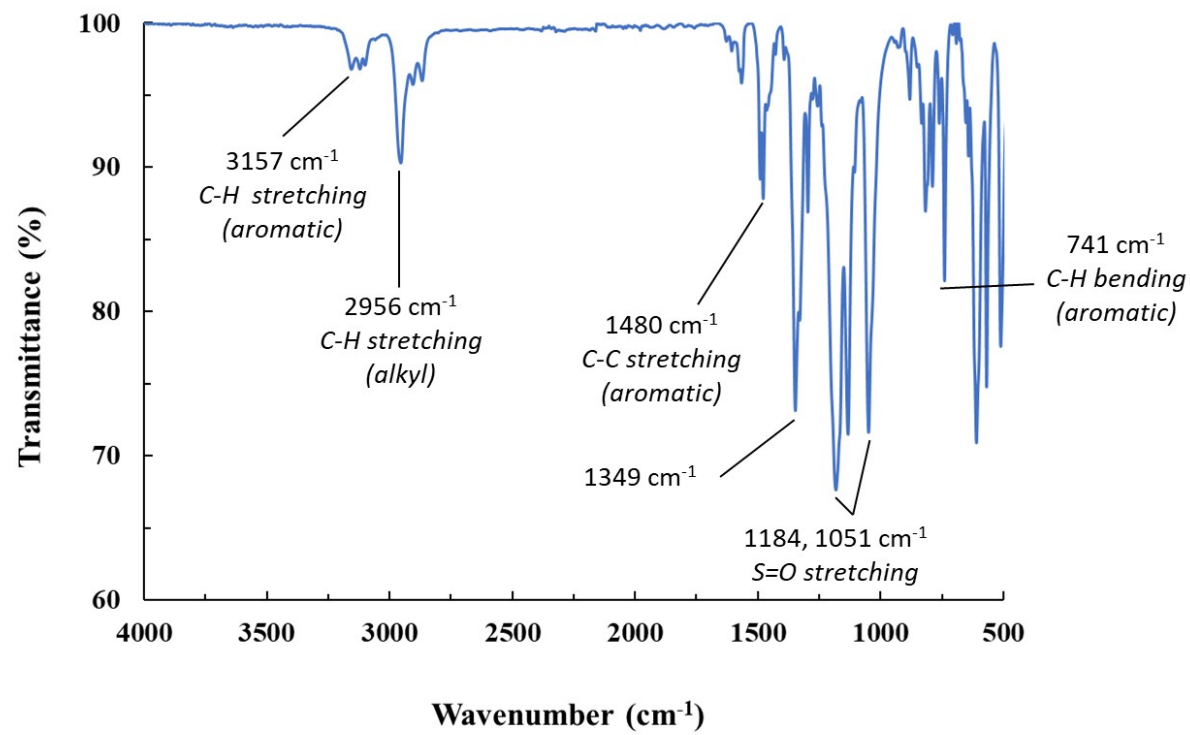
3157; 2956; 1480; 1184; 1051; 741 cm^{-1}

Figure 23 FTIR spectra of 3-(2-(3,6-di-*tert*-butyl-9*H*-carbazol-9-yl)ethyl)-1-methyl-1*H*-imidazol-3-ium *TFSI* (***T-cation***)
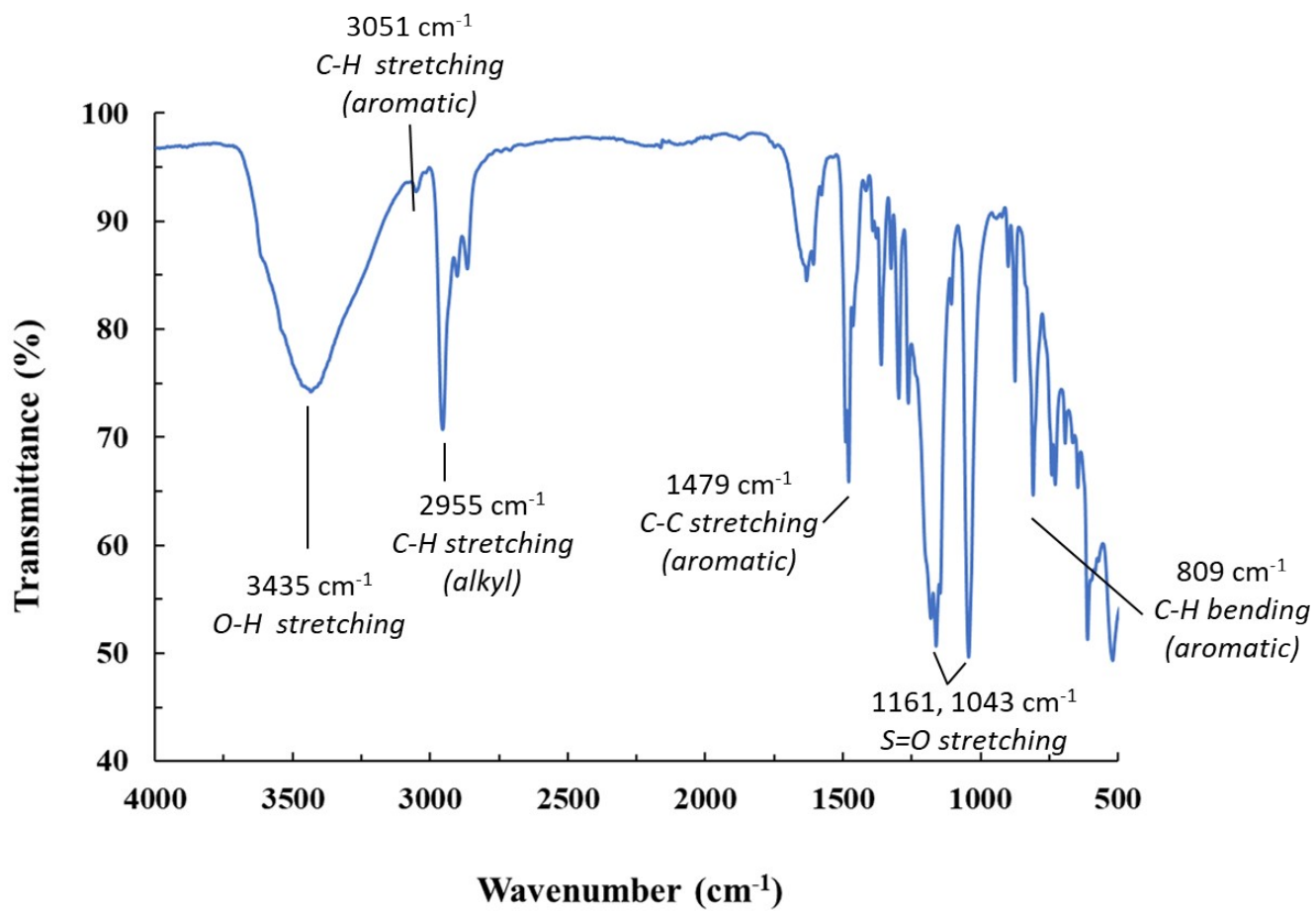
3435; 3051; 2955; 1479; 1161; 1043; 809 cm^{-1}

Figure 24 FTIR spectra of 3-(3,6-di-*tert*-butyl-9*H*-carbazol-9-yl)propane-1-sulfonate

100

90

80

Transmittance (%)

70

60

O-H
stretching

50

2959 cm^{-1}
C-H stretching
(alkyl)

3041 cm^{-1}

40

C-H stretching
(aromatic)

1660 – 1480 cm^{-1}
C-C stretching
(aromatic)

30

1321 cm^{-1}

808 cm^{-1}
C-H bending
(aromatic)

1181, 1069cm^{-1}
S=O stretching

20

4000   3500   3000   2500   2000   1500   1000   500

Wavenumber (cm^{-1})
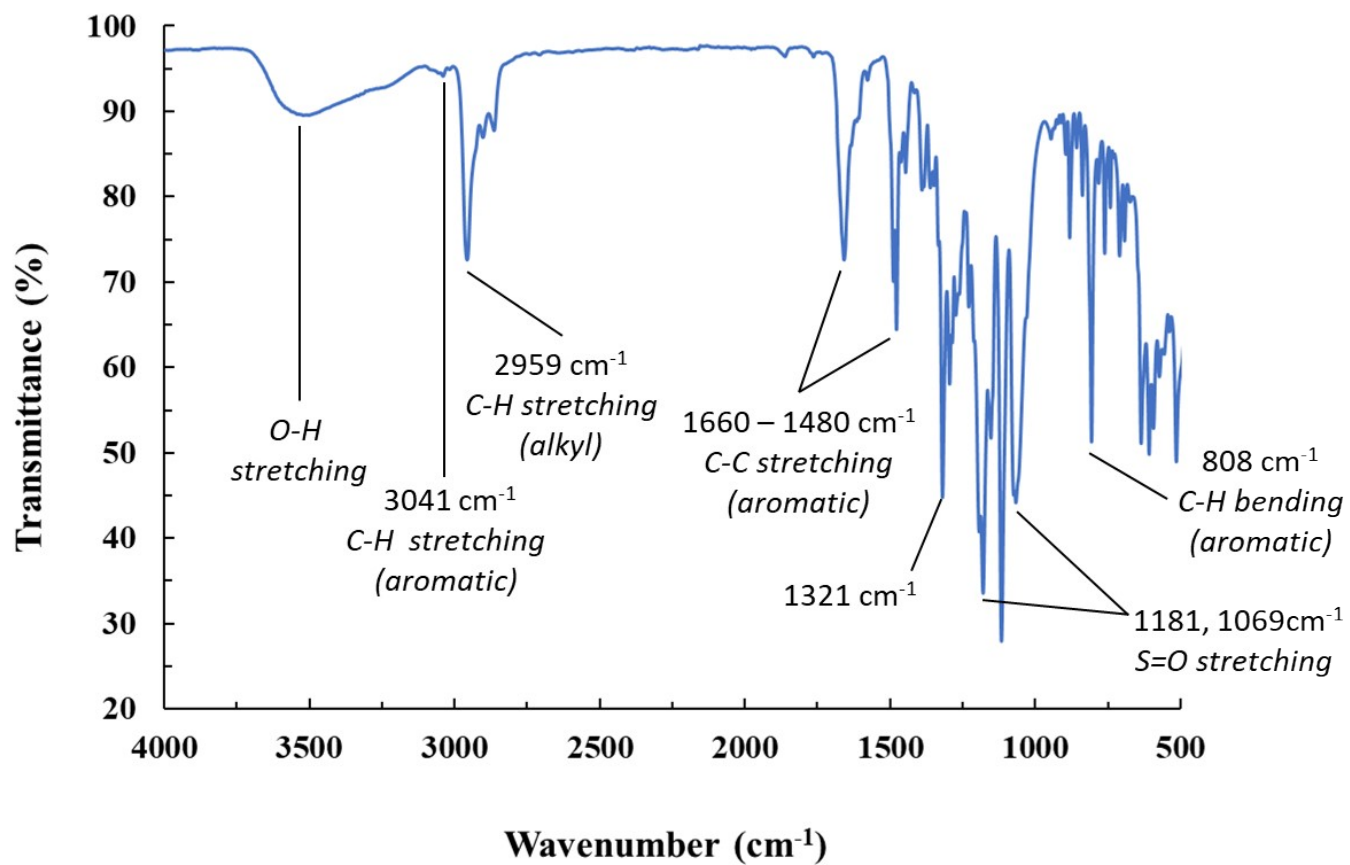
3041; 2959; 1660−1480; 1321; 1181; 1069; 808 cm^{-1}

Figure 25 FTIR spectra of Lithium ((3-(3,6-di-*tert*-butyl-9*H*-carbazol-9-yl) propyl)sulfonyl) ((trifluoromethyl)sulfonyl)amide

100

Transmittance (%)

90

3079 cm^{-1}
C-H stretching
(aromatic)

2957 cm^{-1}
C-H stretching
(alkyl)

1481 cm^{-1}
C-C stretching
(aromatic)

808 cm^{-1}
C-H bending
(aromatic)

cm^{-1}
S=O stretching

1168, 1058 cm^{-1}
S=O stretching

4000   3500   3000   2500   2000   1500   1000   500

Wavenumber (cm^{-1})
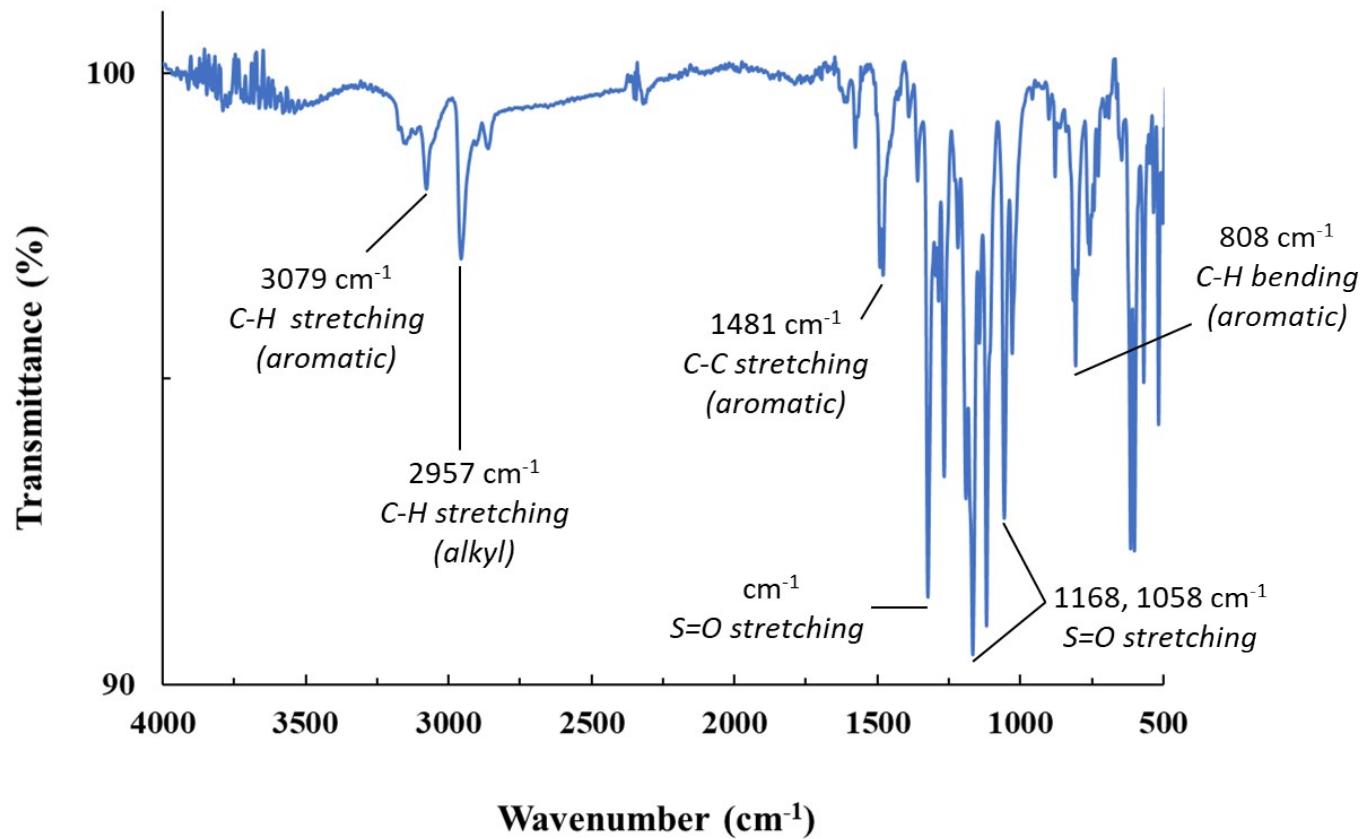
3079; 2957; 1481; 1168; 1058; 816 cm^{-1}

Figure 26 FTIR spectra of 3-ethyl-1-methyl-1*H*-imidazol-3-ium ((3-(3,6-di-*tert*-butyl-9*H*-carbazol-9-yl)propyl)sulfonyl)((trifluoromethyl)sulfonyl)amide (**T-anion**)
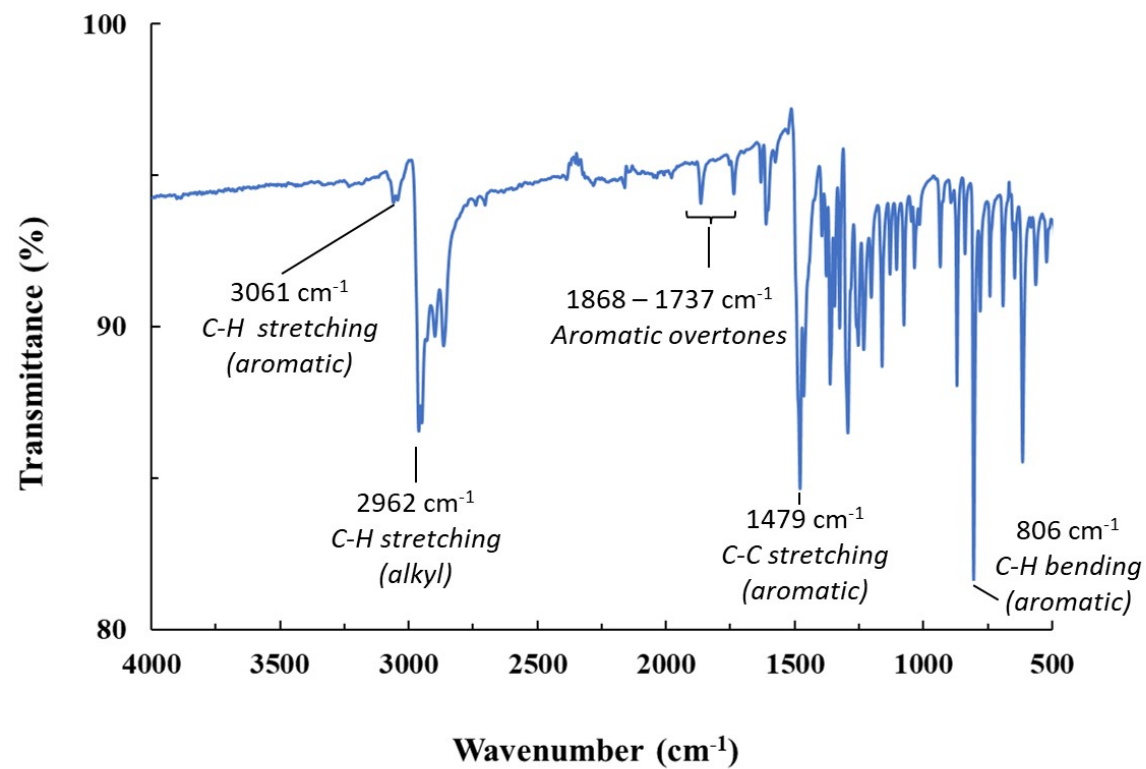
3061; 2962; $1868-1737$; 1479; 806 cm^{-1}

Figure 27 FTIR spectra of 3,6-di-*tert*-butyl-9-ethyl-9*H*-carbazole (***T-standard***)

Thermogravimetry analysis (TGA) and Differential thermal analysis (DTA)

Figure 28 TGA and DTA of 3-(2-(3,6-di-*tert*-butyl-9*H*-carbazol-9-yl)ethyl)-1-methyl-1*H*-imidazol-3-ium *TFSI* (***T-cation***)

Figure 29 TGA and DTA of 3-ethyl-1-methyl-1*H*-imidazol-3-ium ((3-(3,6-di-tert-butyl-9*H*-carbazol-9-yl)propyl)sulfonyl)((trifluoromethyl)sulfonyl)amide (***T-anion***)
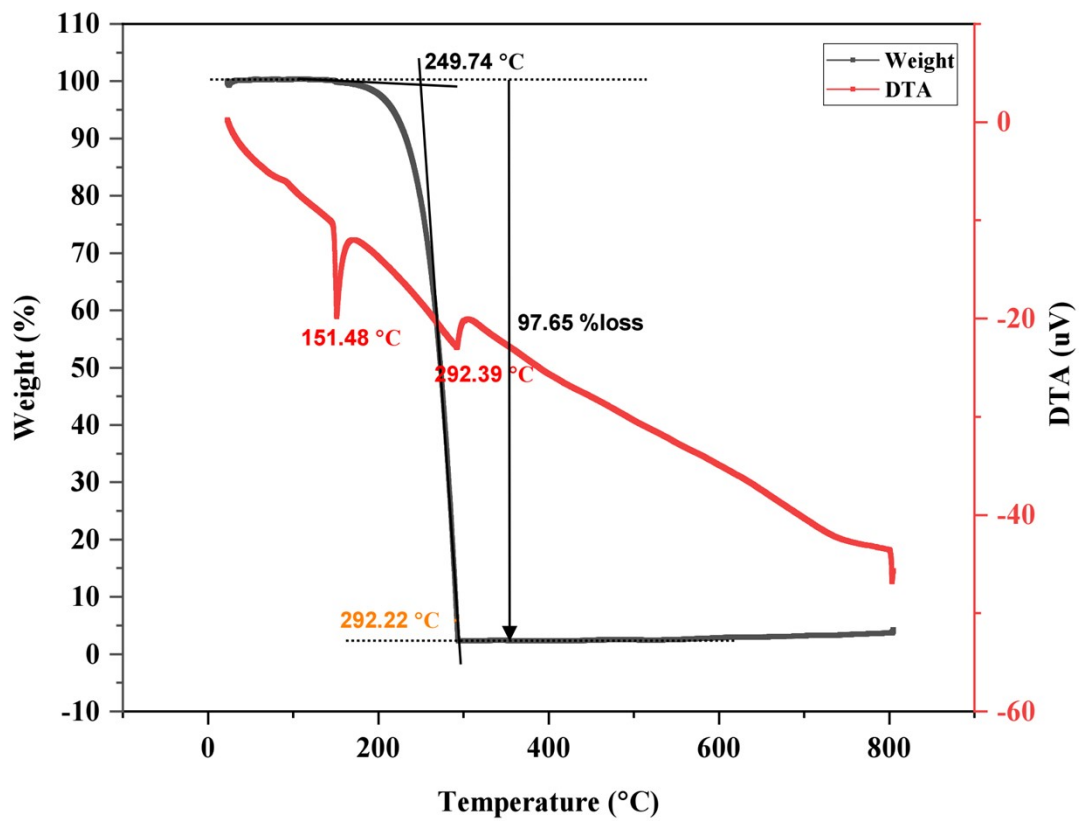
Figure 30 TGA and DTA of 3,6-di-*tert*-butyl-9-ethyl-9*H*-carbazole (***T-standard***)

Differential scanning calorimetry (DSC)

Figure 31 DSC of 3-(2-(3,6-di-*tert*-butyl-9*H*-carbazol-9-yl)ethyl)-1-methyl-1*H*-imidazol-3-ium

TFSI (***T-cation***)
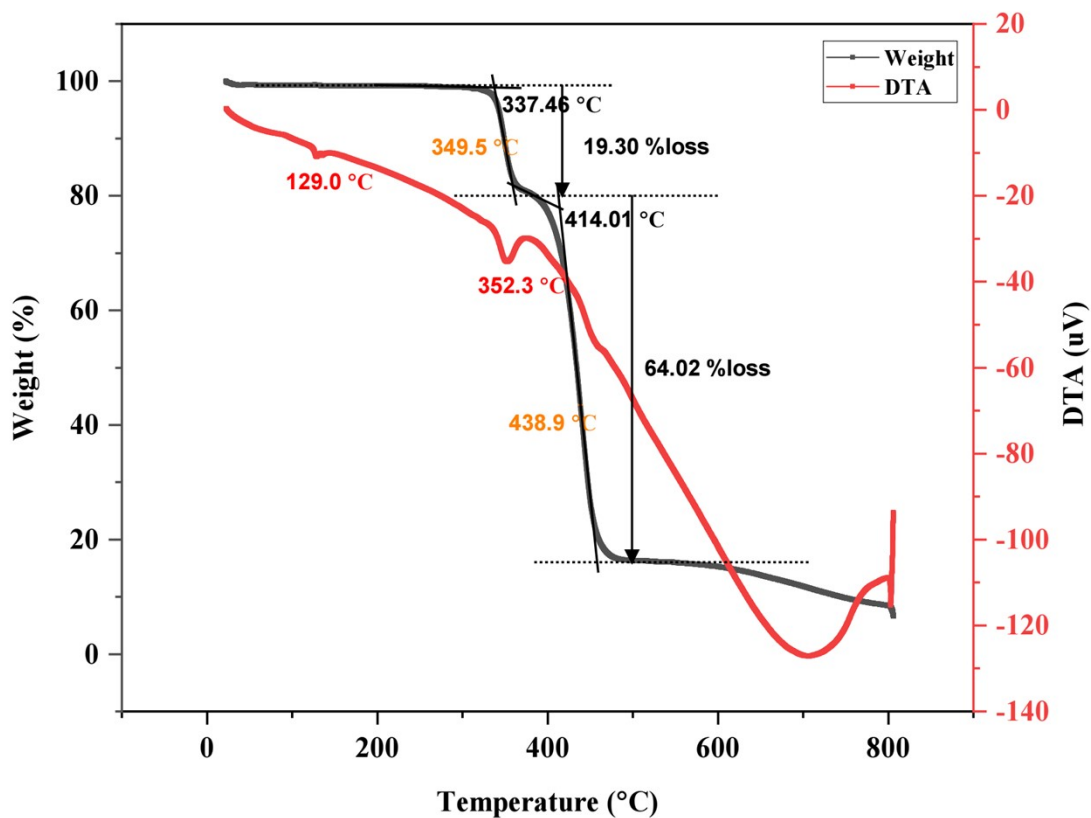
Figure 32 DSC of 3-ethyl-1-methyl-1*H*-imidazol-3-ium ((3-(3,6-di-tert-butyl-9*H*-carbazol-9-yl)propyl)sulfonyl)((trifluoromethyl)sulfonyl)amide (***T-anion***)
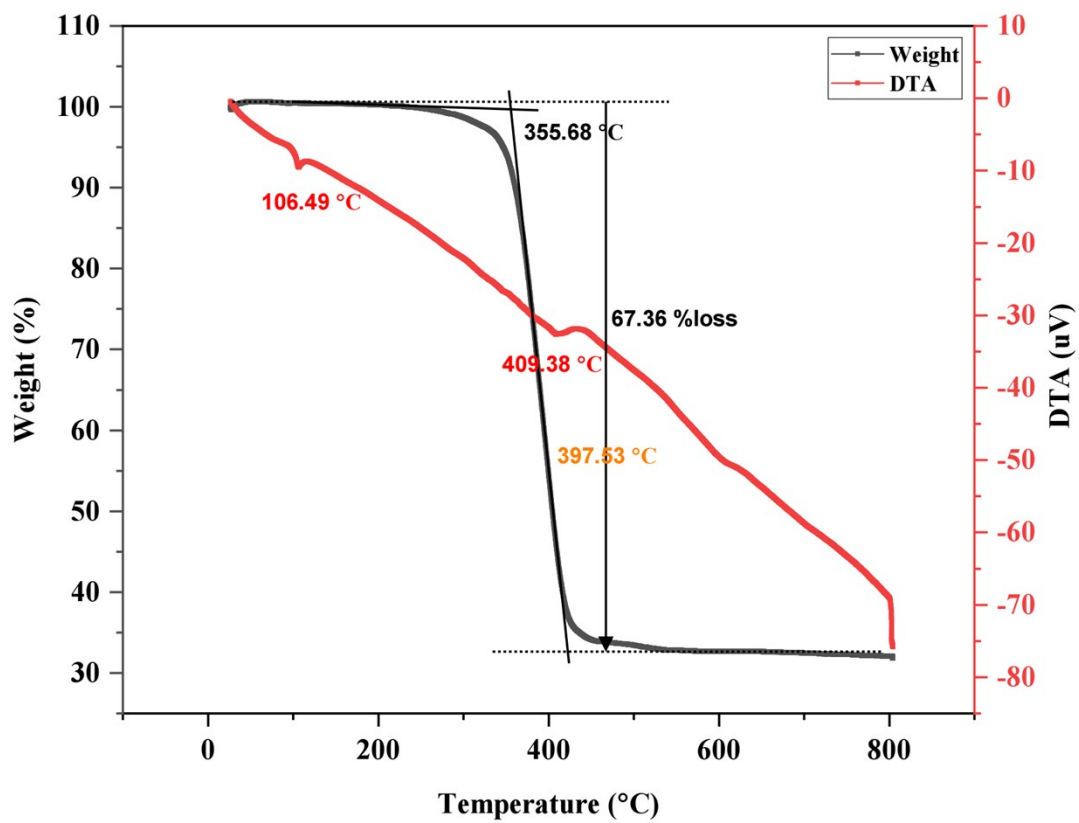
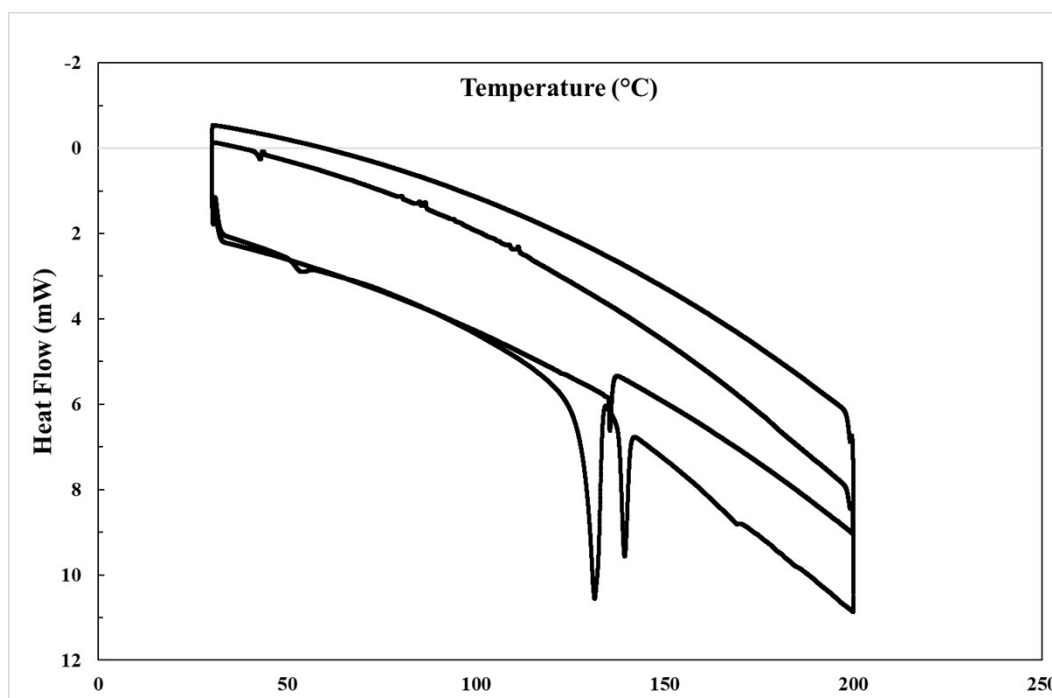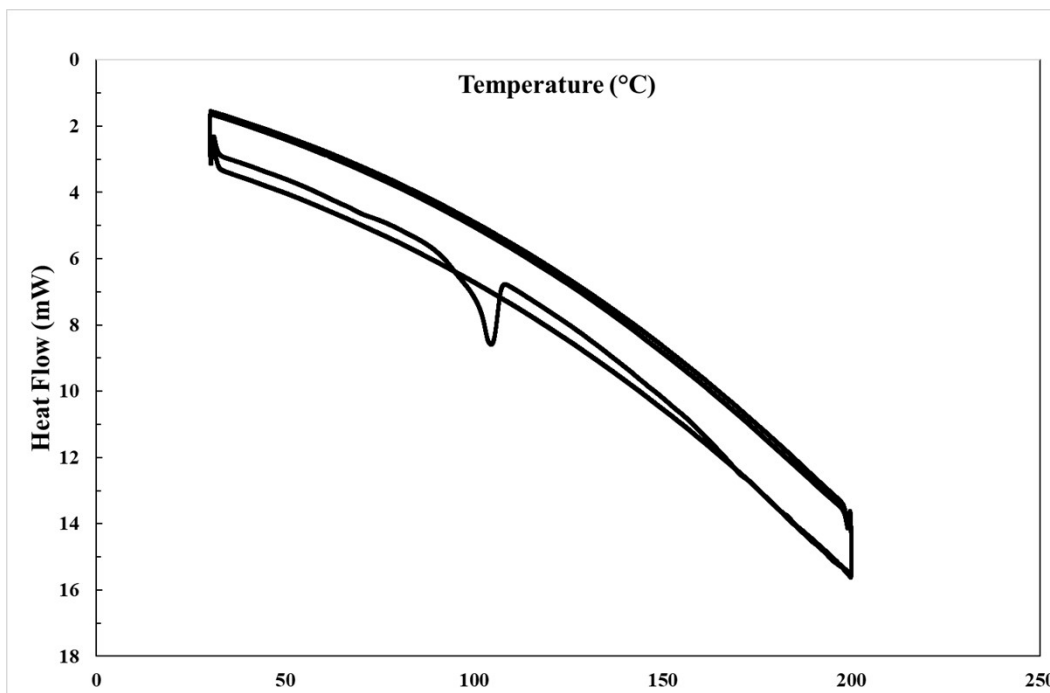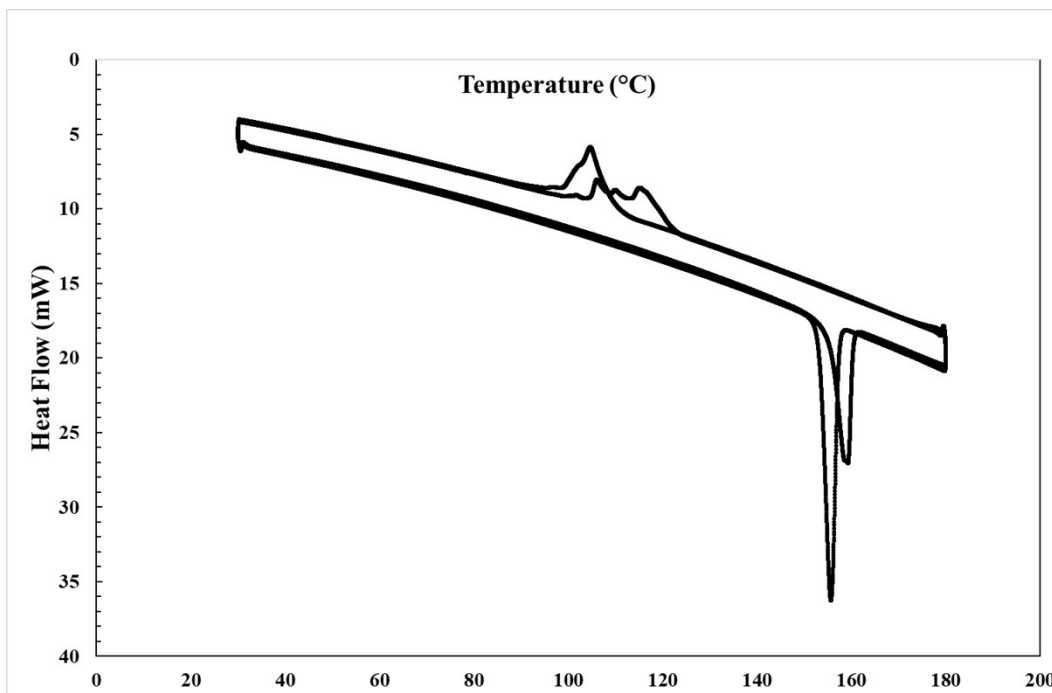**Figure 33** DSC of 3,6-di-*tert*-butyl-9-ethyl-9*H*-carbazole (***T-standard***)

Mass Transport

Diffusion coefficient of oxidized form/(cm²s⁻¹)		
	CVs with millimeter-sized electrode	CA with micrometer-sized electrode
Ferrocene	2.5×10^{-7}	2.7×10^{-7}
FcEmi*TFSI*	1.4×10^{-7}	1.7×10^{-7}

S 14 Values of the diffusion coefficient for FcEmi*TFSI* and Ferrocene in Emi*TFSI* obtained by various electrochemical technique (O. Fontaine et al. / Journal of Electroanalytical Chemistry 632 (2009) 88-96)

By comparing the value of diffusion coefficient of the references and the carbazole derivatives in this experiment, both diffusion coefficient values are considered related in the same range.

| Kinetic Rate		
Molecule	K^0_{app} with CVs /(cm s⁻¹)	K^0_{app} with EIS /(cm s⁻¹)
Ferrocene	$(2.1 \pm 0.3)^{-2}$	$(1.0 \pm 0.2)10^{-2}$
FcEmiTFSI	$(0.5 \pm 0.1)^{-2}$	$(0.5 \pm 0.1)^{-2}$

S 15 Values of the kinetic rate for FcEmi*TFSI* and Ferrocene in Emi*TFSI* obtained by various electrochemical technique. (O. Fontaine et al. / Journal of Electroanalytical Chemistry 632 (2009) 88-96)

The value of kinetic rate of the reference and the carbazole derivatives are in comparison in the same range at 10^{-2}.

Molecule	Diffusion Coefficient (cm²·s⁻¹)	Diffusion Coefficient (cm²·s⁻¹) (From UME)	E⁰ Value vs Ag/AgCl (V)	E⁰ Value vs Ag/AgCl (V) (From UME)	R solvation (Å)	k⁰ (cm·s⁻¹)
T-anion	$1.64 \cdot 10^{-5}$	$2.83 \cdot 10^{-5}$	1.43	1.52	3.5	1.83
T-cation	$5.62 \cdot 10^{-6}$	$9.26 \cdot 10^{-5}$	1.32	1.29	8.1	1.51
T-standard	$1.64 \cdot 10^{-5}$	$5.82 \cdot 10^{-5}$	1.21	1.30	3.0	0.96

S 16 Values of the diffusion coefficient (cm² ·s⁻¹) for the 3 molecules, E^0 (V) value, the solvation radius (Å) and the apparent rate constant $k^{\,0}$ (cm² ·s⁻¹) determined by *CVs* millimeter-sized electrode and ultramicro-electrode (*UME*).

Cation	$D/\text{cm}^2 \cdot \text{s}^{-1}$	$r_{solv}/\text{Å}$	$r_{unsolv}/\text{Å}$	$k_0/\text{cm} \cdot \text{s}^{-1}$	$r_{ET}/\text{Å}$
1	1.56×10^{-6}	40	13	0.2	14
2	4.53×10^{-6}	16	8	1.4	8
TEMPO	1.22×10^{-5}	4	4	2	4
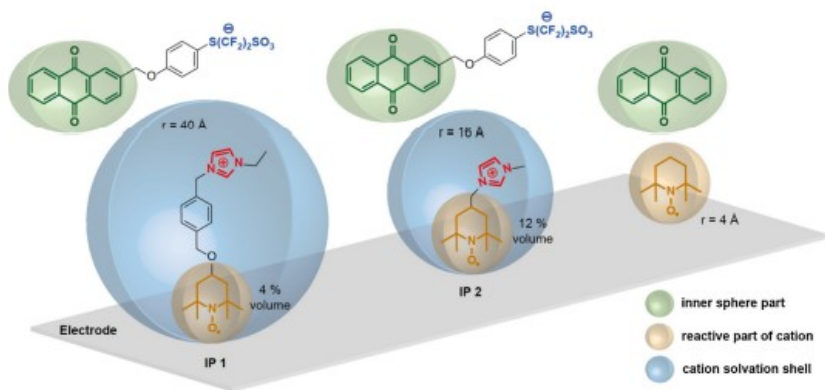
S 17 Reference value and schematic representation of likely preferential orientation of the TEMPO bearing species A, B and C during electron transfer and the sizes of the cation solvation shells
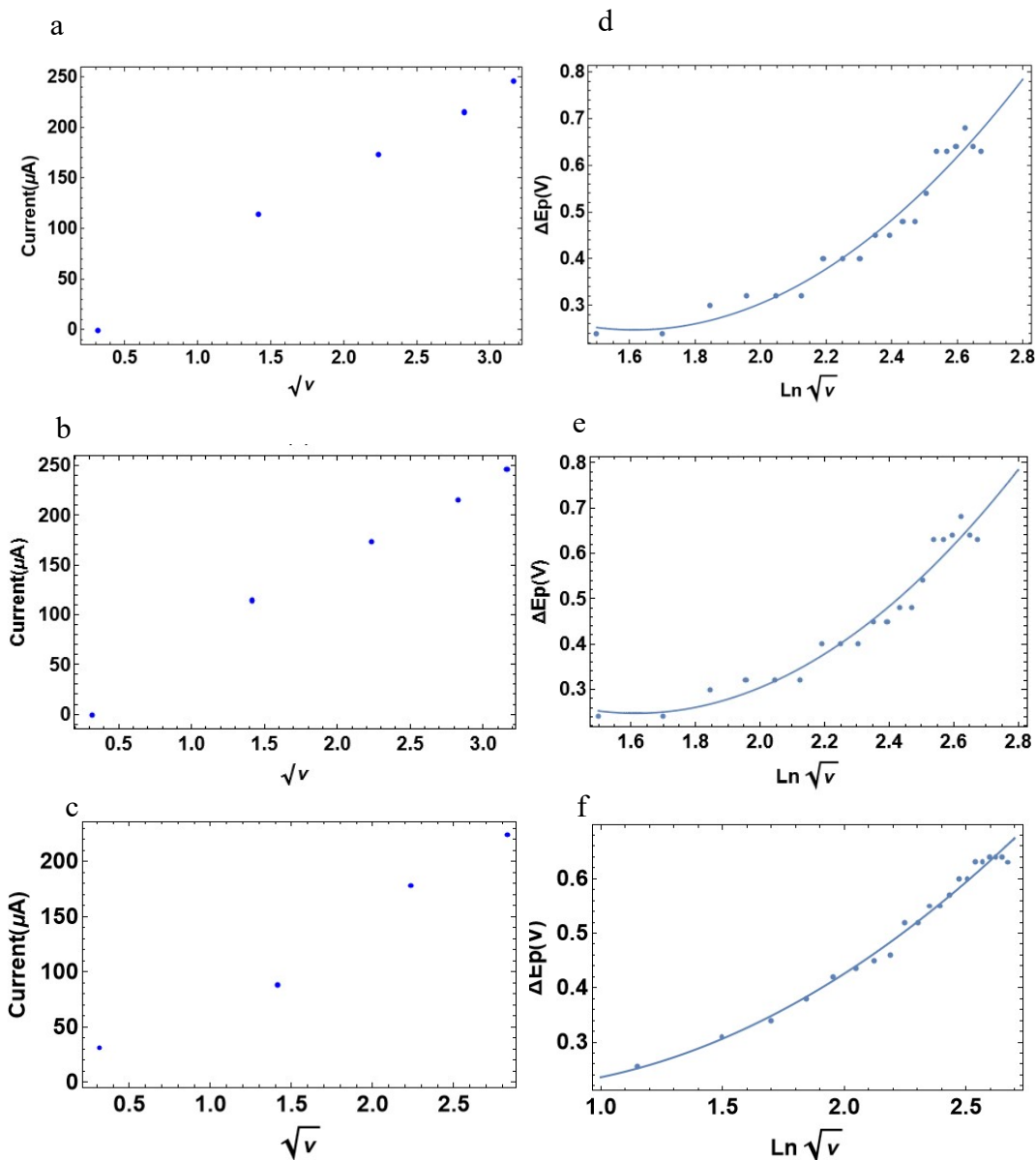
rsolv and the reactive parts of the cation from E. Mourad et al. / Electrochimica Acta 206 (2016) 513–52

S 18 The graphs represent the plot between current ratio and square root of scan rate of a.) *T-anion*, b.) *T-cation*, and c.) *T-standard*. The kinetic rate of electron transfer represented peak-to-peak separation and Ln of square root scan rate d.) *T-anion*, e.) *T-cation*, and f.) *T-standard*
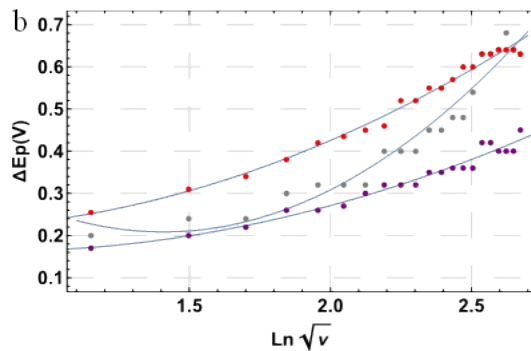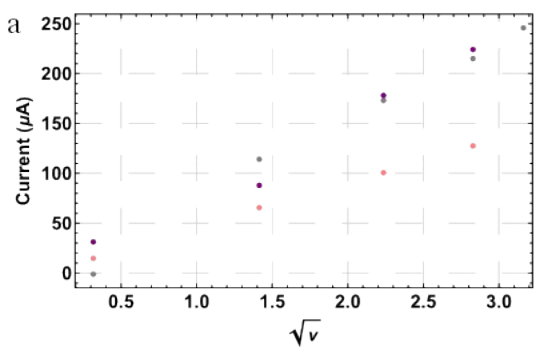
S 19. (a.) Variation the anode $i_{p,a}$ currents as a function of the square root of the scan rate of molecule *T-standard* , (b.) Variation of the peak-to-peak separation ΔEp as a function of ln $v^{1/2}$

Variation the anode $i_{p,a}$ currents as a function of the square root of the scan rate of molecule example from *T-standard.*
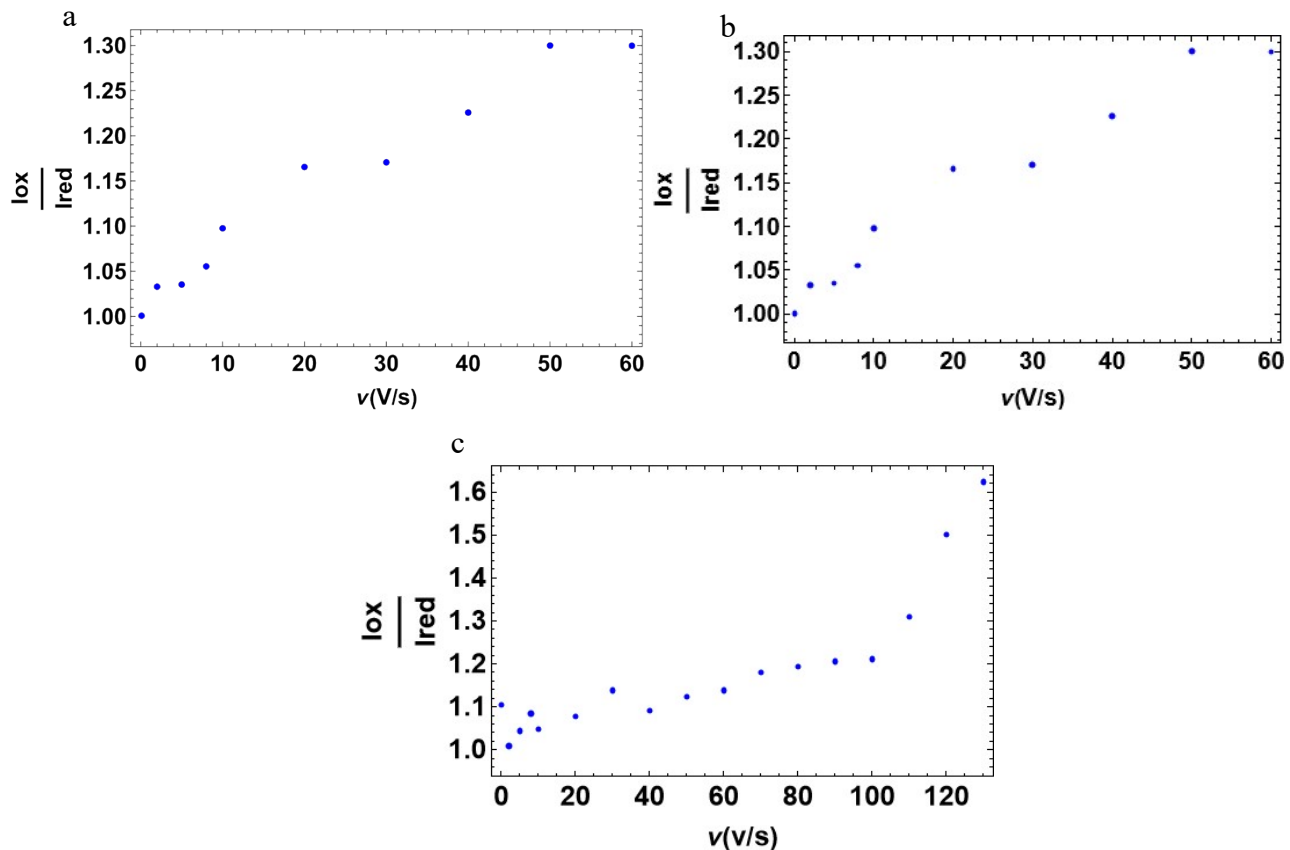
S 20 The plot represents the current ratio vs the varied scan rate a.) *T-anion*, b.) *T-cation*, and c.)

T-standard

$$i = \frac{(1 - (B \cdot (E_1 - E_0))) - (A \cdot Exp[\frac{\alpha \cdot F}{R \cdot T} \cdot (E_1 - E_0)]) \cdot i_0}{1 + (\frac{1}{RKN}) \cdot (Exp[\frac{\alpha \cdot F}{R \cdot T} \cdot (E_1 - E_0)] \cdot \frac{1}{RKN})}$$

$$\frac{1}{RKN} = (\frac{\frac{D}{k^0 \delta}}{)}$$

S 21 Steady-state cyclic voltammetry fitted using Wolfram Mathematica. The equation for fitting the curve obtained by using the fabricated ultra-microelectrode. This equation is modified from the steady-state curve fitted equation.

E_0 is Formal Potential (v), α is anodic transfer coefficient, F is faraday constant, i_0 is current limit (when $E_1=E_0$), T is temperature (K), R is Gas constant, k^0 is Heterogeneous rate constant, δ is the diffusion layer thickness and D is the diffusion coefficient.

T-cation
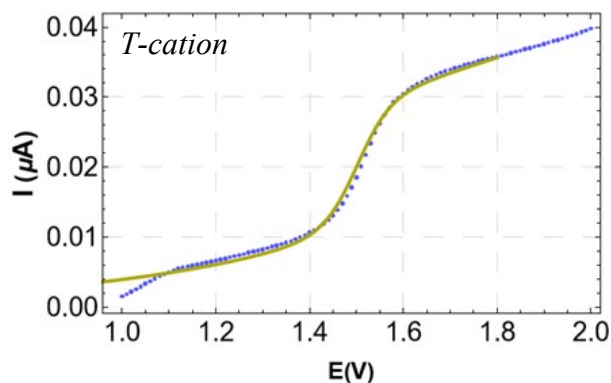
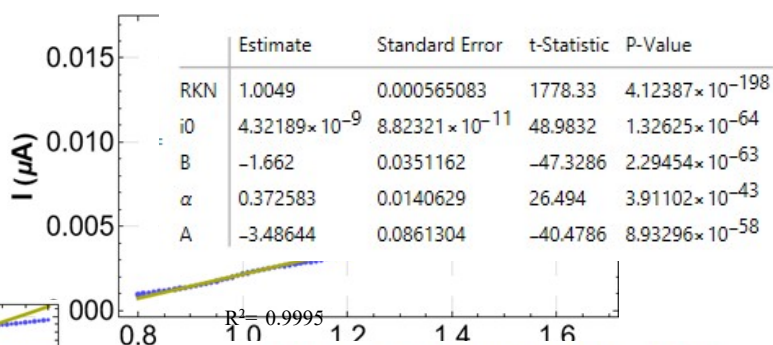|	Estimate	Standard Error	t-Statistic	P-Value
RKN	0.922988	0.00530443	174.003	7.9408×10^{-122}
i0	2.91408×10^{-8}	3.57118×10^{-10}	81.5998	1.74243×10^{-90}
B	−0.743829	0.044902	−16.5656	6.68261×10^{-30}
α	−0.251355	0.0187473	−13.4075	1.00841×10^{-23}
A	−0.431347	0.020053	−21.5104	1.71513×10^{-38}

$R^2 = 0.9992$

T-anion

	Estimate	Standard Error	t-Statistic	P-Value
RKN	1.0049	0.000565083	1778.33	4.12387×10^{-198}
i0	4.32189×10^{-9}	8.82321×10^{-11}	48.9832	1.32625×10^{-64}
B	−1.662	0.0351162	−47.3286	2.29454×10^{-63}
α	0.372583	0.0140629	26.494	3.91102×10^{-43}
A	−3.48644	0.0861304	−40.4786	8.93296×10^{-58}

$R^2 = 0.9995$
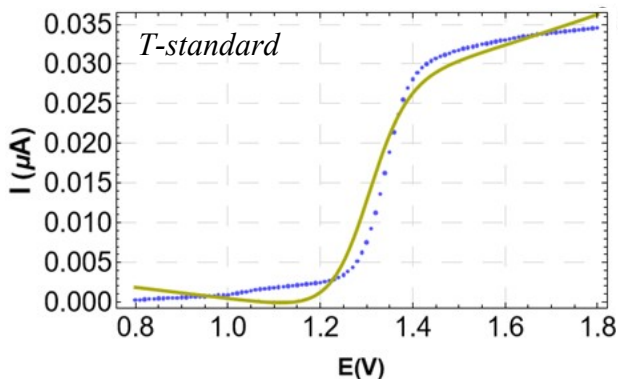
T-standard

	Estimate	Standard Error	t-Statistic	P-Value
RKN	0.851002	0.00702803	121.087	8.84579×10^{-107}
i0	3.04651×10^{-8}	1.6321×10^{-10}	186.662	9.56419×10^{-125}
B	−0.315948	0.0199032	−15.8743	1.35444×10^{-28}
α	−0.350373	0.0115664	−30.2923	6.27756×10^{-51}
A	−0.283903	0.0126346	−22.4702	5.16143×10^{-40}

$R^2 = 0.9997$
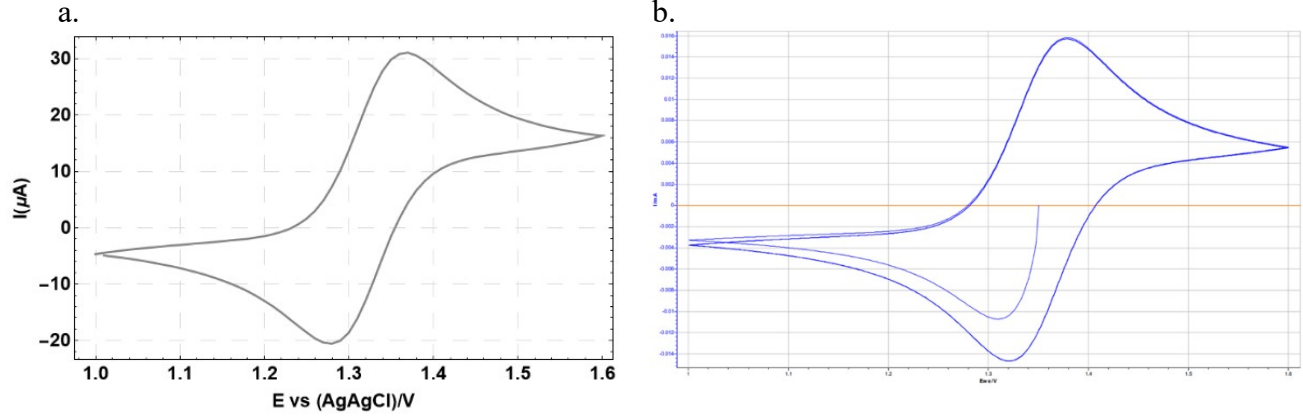
S 22 Electrochemical characterization of *RILs*. The Cyclic voltammetry of *T-cation*, *T-anion* and *T-standard* were dissolved in 2mM ACN with 0.1 M LiClO$_4$. 25μm-platinum ultra-microelectrode was used as the working electrode, Ag wire as reference electrode and platinum as counter electrode. The *CVs* of molecule *T-cation* (a) The *CV* at scan rate 0.05 V/s, The *CVs* of molecule

T-anion (b) The *CV* at scan rate 0.05 V/s, the *CVs* of molecule *T-standard* (c) The *CV* at scan rate 0.05 V/s. Steady-state cyclic voltammetry fitted using Wolfram Mathematica

Where E^0 is Formal Potential (V), α is anodic transfer coefficient (dimensionless), F is faraday constant, i_0 is current limit (A, when $E^1=E^0$), T is temperature (K), R is Gas constant, k^0 is Heterogeneous rate constant (cm·s^{-1}), δ is the diffusion layer thickness (m) and D is the diffusion coefficient (cm^2·s^{-1}). The equation for fitting the curve obtained by using the fabricated ultra-microelectrode where the green line is from data and the blue dot is the fitting plot. This equation is modified from the steady-state curve fitted equation. The cyclic voltammetry was also conducted using ultra-microelectrode (Figure 9) [15-19] at the scan rate 0.05 V/s. The steady-state signal was observed using the *UME* on all 3 molecules. The oxidation and reduction peak range of molecule are agreed using the *UME* and millimetric electrode (Figure 8).
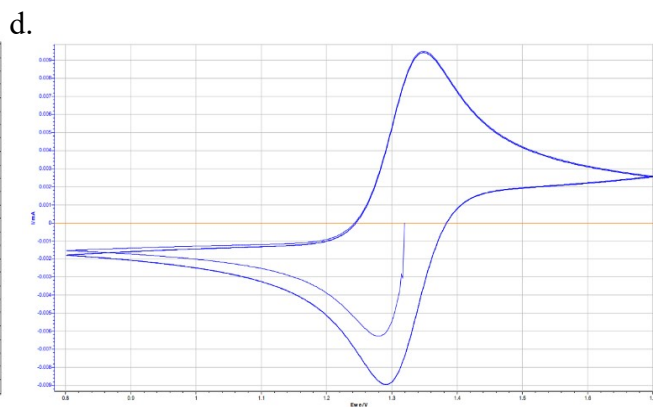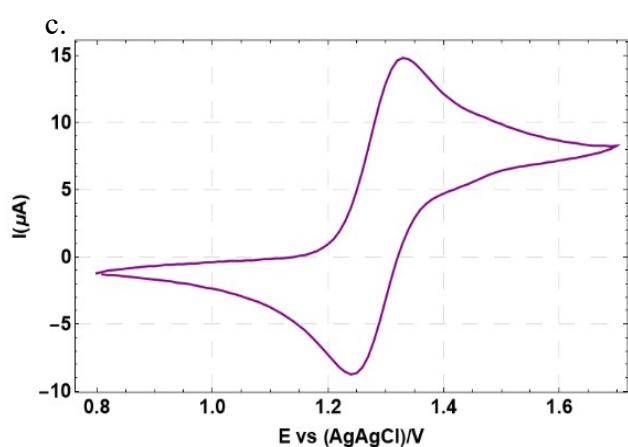
Simulation by EC-Lab software

T-anion

a.

b.

Species:	Setup:	Experimental Conditions:		
CA initial = 2e-3 mol.L^{-1}	Electrode:	Temperature = 25 deg		
CB initial = 2e-3 mol.L^{-1}	Geometry = Linear Semi-infinite	Rohm = 0 Ohm		
DA = 16.4e-6 cm2.s^{-1}	Radius = 3.63 mm	double layer capacitance = 0 uF		
DB = 16.4e-6 cm2.s^{-1}	Surface = 41.4 mm^2	Potential Scan:		
Potential Scan (perform 3 cycles):	Sampling:	Noise:		
Scan type = Linear	Number of points per scan = 800	Add noise = No		
Scan rate = 0.1 V.s^{-1}	Total number of points ~ 2398	Noise level = 0 mA, 0 mV		
Einit = 1.35 V	Sampling time = 7.509 ms			
E1 = 1 V	Potential steps = 0.751 mV			
E2 = 1.6 V				

T-cation

c.

d.

Species:	Setup:	Experimental Conditions:
CA initial = 2e-3 mol.L^{-1}	Electrode:	Temperature = 25 deg
CB initial = 2e-3 mol.L^{-1}	Geometry = Linear Semi-infinite	Rohm = 0 Ohm
DA = 5.62e-6 cm^2.s^{-1}	Radius = 3.63 mm	double layer capacitance = 0 uF
DB = 5.62e-6 cm^2.s^{-1}	Surface = 41.4 mm^2	
Potential Scan (perform 3 cycles):	**Sampling:**	**Noise:**
Scan type = Linear	Number of points per scan = 800	Add noise = No
Scan rate = 0.1e-3 V.s^{-1}	Total number of points ~ 2398	Noise level = 0 mA, 0 mV
Einit = 1.32 V	Sampling time = 15018.774 ms	
E1 = 1 V	Potential steps = 1.502 mV	
E2 = 1.6 V		

T-Standard
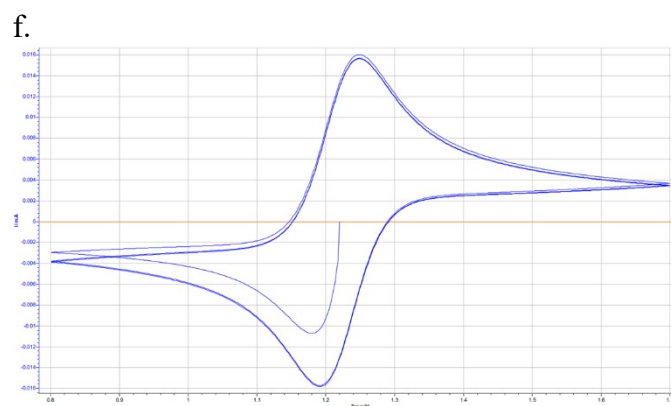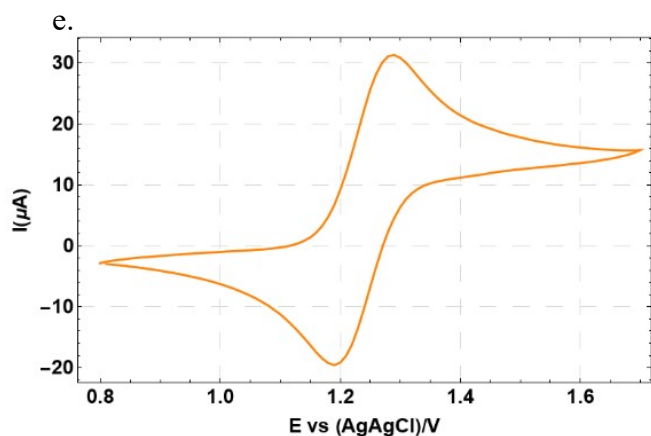
Species:	Setup:	Experimental Conditions:
CA initial = 2e-3 mol.L^{-1}	Electrode:	Temperature = 25 deg
CB initial = 2e-3 mol.L^{-1}	Geometry = Linear Semi-infinite	Rohm = 0 Ohm
DA = 16.4e-6 cm^2.s^{-1}	Radius = 3.63 mm	double layer capacitance = 0 uF
DB = 16.4e-6 cm^2.s^{-1}	Surface = 41.4 mm^2	
Potential Scan 3 cycles :	**Sampling:**	**Noise:**
Scan type = Linear	Number of points per scan = 800	Add noise = No
Scan rate = 0.1e-3 V.s^{-1}	Total number of points ~ 2398	Noise level = 0 mA, 0 mV
Einit = 1.22 V	Sampling time = 22528.162 ms	
E1 = 0.8 V	Potential steps = 2.253 mV	
E2 = 1.7 V		

S 23 The cyclic voltammetry of T-anion (a), T-cation (c), and T-standard (e) obtained from experiment, the simulation peak of T-anion (b), T-cation (d), and T-standard (f) from the EC-Lab software. The table obtained from EC-Lab software represents the value of the diffusion coefficient calculated using the Randles-Sevcik equation.

The simulated cyclic voltammetry of T-anion (b), T-cation (d), and T-standard (f) from the EC-Lab software. The software simulated the curve using the diffusion coefficient which was calculated using Randles-Sevcik equation, and kinetic constant analyzed by Nicholson and Chain. The software simulated using value from the calculation, show the accurate characteristic with the experiment.

References

1.	Rit, A., T. Pape, and F.E. Hahn, *Self-Assembly of Molecular Cylinders from Polycarbene Ligands and AgI or AuI.* Journal of the American Chemical Society, 2010. **132**(13): p. 4572-4573.

2.	Bogdal, D., et al., *Development of Carbazole and Bipyridine Copolymers as Novel Photovoltaic Materials.* Macromolecular Symposia, 2008. **268**(1): p. 110-114.

3.	Chen, Y., et al., *A new method for improving the conductivity of alkaline membrane by incorporating TiO2- ionic liquid composite particles.* Electrochimica Acta, 2017. **255**: p. 335-346.

4.	Zheng, S. *Selectively permeable graphene oxide membrane*. 2016; Available from: https://patents.google.com/patent/WO2017106540A1/en.

5.	Ameen, S., et al., *Diphenylaminocarbazoles by 1,8-functionalization of carbazole: Materials and application to phosphorescent organic light-emitting diodes.* Dyes and Pigments, 2016. **124**: p. 35-44.